JPRS-UPM-91-007
3 DECEMBER 1991

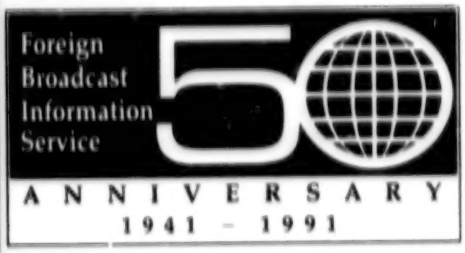

JPRS Report

Science & Technology

USSR: Physics & Mathematics

Science & Technology
USSR: Physics & Mathematics

JPRS-UPM-91-007 CONTENTS *3 December 1991*

Acoustics

Crystals, Laser Glasses, Semiconductors

Lasers

Magnetohydrodynamics

Nuclear Physics

Optics, Spectroscopy

Plasma Physics

Superconductivity

Thermodynamics

Theoretical Physics

Microwave Testing of $Mn_{1-x-y}Cd_xMn_xTe$ Semiconductor

927J0002D Kiev UKRAINSKIY FIZICHESKIY ZHURNAL in Russian Vol 36 No 7, Jul 91 pp 1115-1119

[Article by V. D. Prozorovskiy, I. Yu. Reshidova, S. Yu. Paranchich, and L. D. Paranchich, Donetsk Institute of Engineering Physics at UkSSR Academy of Sciences and Chernovtsy University]

UDC 621.315.592.3

[Abstract] An experimental study of the zero-gap semiconductor $Hg_{1-x-y}Cd_xMn_yTe$ with x = 0.057 and y = 0.023 was made concerning propagation of Alfven waves through single crystals of this material in a magnetic field at temperatures covering the 1.55-6 K range. Specimens of such crystals were grown by the Bridgman method in the form of 0.6-0.8 mm thick disks 5.0-5.5 mm in diameter and then annealed in Hg vapor. Their chemical composition and homogeneity were monitored with the aid of a COMEBAX x-ray microanalyzer directly indicating the Cd content and on the basis of the Electron-Paramagnetic Resonance spectra indicating the Mn content. The intensity of EPR absorption lines was measured at 100-130 K temperatures, the electrical conductivity of all tested specimens being at these temperatures approximately the same as that of the reference specimen. The derivative of the reflection coefficient with respect to the magnetic field intensity dR/dB was measured with a microwave spectrometer in Faraday and Voigt configurations, its absorption-type resonator cavity having been tuned to a frequency of 36.4 GHz. The dependence of this derivative on the magnetic field intensity was found to be an oscillatory one in both configurations, evidently owing to propagation of Alfven waves through such a crystal and thus corresponding to Fabry-Perot resonances. The mobility $\mu_{e,p}$ and the relative effective mass $m_{e,p}^*/m_0$ (m_0) on the basis of available experimental data, for a determination of their temperature dependence. The results indicate small effective electron and hole masses of the same order of magnitude, also nonresonant cyclotron absorption of the Alfven waves by electrons with positive and negative effective masses. This evidence is consistent with the Pashitskiy-Bratashevskiy-Prozorovskiy-Nikolayev model of energy bands, which takes into account hybridization of bands and formation of electron-hole exciton pairs in a dielectric or semiconductor. According to this model, the steep dip of both electron mobility and hole mobility within the 1.55-2 K temperature range is attributable to restructurization of the electronic spectrum and breakup of existing donor-acceptor pairs. Figures 4; references 16.

Ergodynamics of Crater Formation by Impact and Principles of Impact Simulation

927J0009B Leningrad PISMA V ZHURNAL TEKHNICHESKOY FIZIKI in Russian Vol 17 No 7, Apr 91 pp 4-9

[Article by A. S. Balankin and G. N. Yanevich]

[Abstract] Various models of crater formation by impact have been constructed for simulation and study purposes, those based on linear nonequilibrium thermodynamics not being adequate for an open far-from-equilibrium system. Two interrelated and competing processes determine the kinetics of such a crater formation, namely adaptation and dissipation of the kinetic energy of the striker in the barrier acquiring it as the striker comes to rest, only the adaptable part of this energy being expended on crater formation. Inasmuch as the energy relaxation time is much longer than the momentum relaxation time in atoms of solid materials, excess energy builds up in the barrier in the vicinity of its contact with the striker and this region of excess energy adaptation becomes an open far-from-equilibrium system. Mass energy transfer to the surrounding target material or also to the ambient medium, depending on the impact velocity, makes this system capable of self-organization. Explosive crater formation by a hypervelocity impact is considered according to M. A. Lavrentyev ("Artificial Earth Satellites", Akad. Nauk SSSR No 3, 1959, No 4, 1960) and K. P. Stanyukovich ("Nonsteady Motions of Continuous Medium", Izd. Nauka, 1971). In this case self-organization of the dissipative structure occurring as any of the controlling parameters (strain, strain rate, mass flow rate) reaches its critical level and, according to the S-theorem (A.S. Balankin ZHURNAL TEKHNICHESKOY FIZIKI Vol 59 No 12, 1989 and PISMA V ZHURNAL TEKHNICHESKOY FIZIKI Vol 15 No 22, 1989; Vol 16 No 7, 1990) is accompanied by an abrupt decrease of entropy S and of entropy production P. Both extreme situations of pseudoelastic and perfectly inelastic impact have been considered by those authors. A multifractal analysis of crater surfaces formed by hypervelocity impact now reveals some analogy between the ergodynamics of explosive hypervelocity impact and the ergodynamics of free crush, except that in the former case energy builds up not within the volume of the barrier but within the region of excess energy adaptation with a fractal structure. The shape of a crater formed by a hypervelocity impact evolves, owing to surface multifractality, and its volume depends on the striker dimensions. Accordingly, there can be formed microcraters, small craters, large craters, and giant craters. The authors thank G. V. Vstovskiy, V. S. Ivanova, N. A. Zlatin, A. V. Kolotilov, A. A. Lyubomudrov, I. T. Sevryukov, G. S. Pugachev, A. Ya. Sagomonyan., A. A. Kozhushko, V. P. Chelyshev, and V. Ye. Khartsiyev for fruitful discussion of pertinent problems, also Ye. I. Shemyakin for pointing out the analogy between free crush and crater formation by impact. Figures 2; references 22.

Nonself-Similar Blast Waves

927J0017A Novosibirsk FIZIKA GORENIYA I VZRYVA in Russian Vol 27 No 3, May-Jun 91 pp 83-91

[Article by S. M. Guirao and G. G. Bach, Ottawa (Canada)

UDC 532.593

[Abstract] Propagation of blast waves which cause explosion depending on the excess pressure as well as on both static and dynamic impulses is analyzed by two perturbation methods and by the density profile method, considering that the propagation of a blast wave passes through three stages of attenuation in terms of intensity and assuming that the conditions for its self-similarity in the high-intensity shock wave stage (radius R_s of the shock wave larger than radius R_i of its energy source but smaller than the dynamic radius R_0 of explosive action, duration of the energy release much shorter than the wave arrival time, and relatively negligible internal energy of the affected charge substance) are not satisfied. The perturbation equations are solved for the excess pressure by expansion with respect to $y = (R_s/R_0)^{j+1}$ according to the J.H.Lee-G.G. Bach method, where $j = 0$ for spherical waves, $j = 1$ for cylindrical waves, $j = 2$ for plane waves, and $R_0 = (E/\pi_0)^{1/(j+1)}$ (E - energy of source, p_0 - ambient pressure) or with respect to $\eta = y/\Sigma_{n=0}^{\infty} A_n y^n$ according to A. Sakurai's method. The density profile is calculated by the W.J. Rae-G.G. Bach-J.H. Lee method, assuming a power-law profile behind the blast wave. Each method yields a somewhat different dependence of the excess pressure Δp_s on the R_s/R_0 ratio. The approximate solutions obtained by these three methods are compared with exact solutions obtained by H.L. Brode's and H. Goldstein-J V. Neumann methods of finite differences. A numerical evaluation of that dependence according to each of these three approximate methods for nonself-similar spherical waves in an inert atmosphere and a comparison of the results with excess pressure versus R_s/R_0 (W.J. Baker) based on experimental data pertaining to explosion of spherical pentolite charges in air at sea level indicate that the density profile method is the most accurate of them over the widest range of blast wave intensity. Figures 3; tables 1; references 26.

Reflection of Oblique Detonation Waves by Metal Substrates

927J0017B Novosibirsk FIZIKA GORENIYA I VZRYVA in Russian Vol 27 No 3, May-Jun 91 pp 126-128

[Article by M. Adamiec, Warsaw (Poland); B. S. Zlobin and A. A. Shtertser, Novosibirsk]

UDC 621.7.044.2

[Abstract] Detonation of double-layer charges on backplates of soft aluminum alloy (RA-2 $\approx$ 45 HV), hard aluminum alloy (RA-6 $\geq$ 100 HV), plain carbon steel, and of single-layer charges on a U-bent aluminum strip was studied by the optical method with an SNYeF-4 (four frames) photographic apparatus recording the shape of detonation wavefronts. This apparatus (made in Poland) consists of an image converter and exposure turn-on cryotrons set for 50 ns exposure time per frame. On the backplates were placed 6-25 mm thick layers of a low-speed explosive charge (15GH3 rock ammonite or rock ammonite + ammonium nitrate in weight ratios 1:2 on aluminum alloy and 1:1 on steel) and on top of such a charge were placed 3-5 mm thick layers of a high-speed explosive trigger charge (cyclonite or PMW-8 plastic). The backplates were struck with detonation waves obliquely incident on their surface from the lower layer (low-speed explosive charge) of this plane-parallel stack at angles feasible in such a configuration with the given trigger charge materials and thus at several angles within the 24-45° range, with impact velocities of 2.6-4.2 km/s (5.3-7.7 km/s in the upper layer). Regular reflection of the detonation waves was always recorded upon their incidence on the two aluminum alloy backplates from 15-25 mm thick ammonite + ammonium nitrate (1:2) charges and upon their incidence on the steel backplate from all 6-25 mm thick ammonite + ammonium nitrate (1:1) charges. Irregular reflection of the detonation waves was recorded upon their incidence on the two aluminum alloy backplates from less than 15 mm thick plain ammonite charges and upon their incidence on the steel backplate from less than 6 mm thick ammonite + ammonium nitrate (1:1) charges. The tests with a U-form charge of 6ZhV ammonite lining the inside surface of a U-bent aluminum strip revealed formation of a Mach cone at the detonation front, with irregular reflection at the bottom of the strip. Figures 1; tables 1; references 8.

Attenuation of Shock Waves by Layers of Homogeneous and Nonhomogeneous Monodisperse Gaseous Suspension and by Layers of Polydisperse One

927J0017C Novosibirsk FIZIKA VYSOKIKH TEMPERATUR in Russian Vol 27 No 3, May-Jun 91 pp 129-134

[Article by A. G. Kutushev and U. A. Nazarov, Tyumen]

UDC 532.529:518.5

[Abstract] Attenuation of shock waves and thus shielding a barrier by layers of homogeneous and nonhomogeneous monodisperse gaseous suspensions of solid particles or by a layer of a polydisperse is considered, such layers lowering the peak pressure at the barrier surface behind the reflected shock wave. A model of a polydisperse gaseous suspension is selected one with two fractions of chemically inert solid particles. Nonsteady one-dimensional flow of such a three-phase medium with attendant interphase interaction and heat exchange are described by a quasi-linear system of partial differential equations formulating the laws of mass and momentum conservation for each phase, the law of total energy conservation within the physical system, and the laws of heat transfer in a generalized notation: indices $i = 1,2,3$ referring respectively to the gaseous carrier phase and the two fractions of the solid phase, indices $j = 2,3$ referring to heat transfer from the gas to those two fractions. In accordance with classical mechanics of

continuous polyphase media, all particles of both fractions are assumed to be spherical (of the same size in the special case of a monodisperse suspension). It is furthermore assumed here that all flow parameters remain constant over distances much larger than the particles and the distances between them, that effects of viscosity and thermal conductivity become appreciable only during interphase interactions, that no deformation, ablation, evaporation of solid particles and no collisions between them occur, and that all changes in the internal energy of the suspended mixture effected by interphase interaction forces including friction and buoyancy are mediated by the gaseous phase. At a time $t = 0$ a shock wave perturbs the gas into forming a ramp profile of its mass flow rate over some finite distance in a horizontal channel, whereupon the shock front passes through a region of quiescent stationary gas followed by a layer of gaseous suspension which is either homogeneous (uniform particle concentration profile, zero concentration gradient) or nonhomogeneous (nonuniform particle concentration profiles, positive or negative concentration gradients) before striking a vertical barrier. The shielding action of such layers is evaluated on the basis of the Rankin-Hugoniot relations for the wavefront in the perturbation region and isentropic process relations for a plain wave with a ramp velocity profile within the rarefaction zone. A numerical analysis reveals that a nonhomogeneous monodisperse layer with a linearly decreasing particle concentration (negative concentration gradient) attenuates a shock wave and thus shields the barrier most effectively, a nonhomogeneous monodisperse layer with a linearly decreasing particle concentration (positive concentration gradient) being least effective and a homogeneous monodisperse layer ranking intermediate in effectiveness. It furthermore reveals that the maximum pressure at the barrier behind a reflected shock wave decreases monotonically with increasing total mass of suspended particles, a shock wave being attenuated more effectively by a layer of homogeneous monodisperse suspension of fine particles than by one of large particles, a polydisperse suspension ranking intermediate in effectiveness. The results of this analysis indicate that, under otherwise identical conditions, shock waves will be attenuated more effectively by monodisperse gaseous suspensions than by polydisperse ones. The authors thank N. A. Gumerov for discussion. Figures 3; references 7.

On New Possibility of Determining Frictional Forces Affecting Dislocation at Its Initial Movement Stage

927J0032B Leningrad FIZIKA TVERDOGO TELA in Russian Vol 33 No 2, Mar 91 pp 763-767

[Article by V. V. Zoninashvili, I. A. Naskidashvili, V. A. Melik-Shakhnazarov, Physics Institute at the Georgian Academy of Sciences, Tbilisi]

[Abstract] The long-range interaction of dislocations with point defects characterized by tetragonal symmetry, e.g., O, N, C interstitial impurities, in body-centered cubic crystalline (OTsK) metals resulting in an orientational defect ordering is discussed. The results of an acoustic investigation of the interaction of dislocations with the polarized atmosphere of oxygen atoms in niobium are cited and it is demonstrated that characteristic minima occur in the process of relaxing the samples whereby the stresses at which the minima are observed differ in magnitude depending on whether they were obtained while loading or relaxing the samples. A mechanical relaxation spectrometer was used to study the samples during their elastic loading in a Snoek atmosphere. The above stress hysteresis is attributed to the effect of frictional forces on the dislocation during its movement. The resulting original method of determining the frictional stresses affecting the dislocation during its initial movement phase and the temperature and velocity dependence of these stresses are consistent with existing concepts. The authors are grateful to Z. K. Saralidze for useful discussions, L. M. Kolesnikova and N. M. Yastrebova for help with the experiments, and V. A. Kocherov, A. M. Uvarov, and I. A. Baglayenko for making the samples. Figures 3; references 7: 3 Russian, 4 Western.

Investigation of Graphite-Diamond Phase Transition Kinetics

927J0040D Moscow TEPLOFIZIKA VYSOKIKH TEMPERATUR in Russian Vol 29 No 3, May-Jun 91 pp 486-493

[Article by A. Z. Zhuk, A. V. Ivanov, G. I. Kanel, High Temperatures Institute at the USSR Academy of Sciences]

UDC 531.3

[Abstract] The history of experimental studies of the impact-initiated graphite-diamond phase transition and the effect of various factors on it are reviewed. The kinetics of the graphite-diamond transition are experimentally investigated. To this end, the graphite's impact compressibility was measured and the dependence of the speed of sound on pressure in the phase transition area was recorded. These measurements were used to estimate the depth of the phase transition. To estimate the pressure of the onset of phase transition and characteristic process duration, the experiment was numerically simulated. Isotropic artificial graphite obtained by the hot molding method at a 3,000K graphitization temperature from KNPS coke and coal tar pitch was used in the experiments. Measurements were taken by manganin pressure transducers. The graphite sample was loaded by the impact of a flat aluminum slab through a duralumin screen or by detonating an explosive charge placed directly in front of the screen. It is noted that the issue of the considerable difference between the pyrolytic graphite and artificial graphite transition to diamond still remains unresolved. It is speculated that the most likely cause is the artificial graphite's higher diffusion activity due to the local heating of structural defects. Figures 8; tables 1; references 26: 18 Russian, 8 Western.

Phase Transformations of Amorphous Binary Semiconductor in Treatment by Laser Pulses

927J0005E Leningrad FIZIKA TVERDOGO TELA in Russian Vol 33 No 1, Jan 91 pp 99-103

[Article by S. Yu. Karpov, Yu. V. Kovalchuk, V. Ye. Myachin, Yu. V. Pogorelskiy, M. Yu. Silova, I. A. Sokolov, and M. I. Etinberg, Institute of Engineering Physics imeni A. F. Ioffe, USSR Academy of Sciences, Leningrad]

UDC 621.315.592

[Abstract] An experimental study of InP, a typical binary semiconductor was made, concerning the formation of its metastable liquid phase during treatment of the material in its amorphous and crystalline initial states. Slices of a (100) InP single crystal were amorphized to an about 80 nm depth by implantation of $5x10^{14}$ cm^{-2} 100 keV Zn^+ ions into one part of such a slice, the other part remaining crystalline. These slices were then treated with 532 nm TEM_{00}-mode radiation from a Q-switched YAG:Nd^{3+} laser in pulses of 25 ns width at 50 percent level. As indicators of the phase transformation dynamics were selected changes in the reflection coefficient for 633 nm s-polarized radiation from a probing He-Ne laser incident at a 24.5° angle. The diameters of the two laser beams were in a $D_{YAG}:D_{He-Ne} \approx 20$ ratio. The error of energy density determination at a point on the semiconductor surface did not exceed about 3 percent and the time resolution of radiation recording was 2 ns or better, the reflection coefficient being measured as a function of time at various levels of the energy density of YAG:Nd^{3+} (melting threshold for amorphous InP) to 400 mJ/cm^2 (surface breakdown threshold for amorphous InP) at the semiconductor surface. The results indicate that changing the initial state of such a semiconductor from crystalline to amorphous "stabilizes" the metastable liquid phase, which can form within a period on the order of 10 ns. Inasmuch as the properties and especially the defectiveness of InP crystals are different depending on whether they have been grown from a stable or unstable melt, this "stabilization" will appreciably influence the properties of ion-implantation layers subsequently annealed by means of laser pulses. Figures 3; references 11.

Ultrasonic Study of Phase Transitions in Multilayer $TlInS_2$ and $TlGeS_2$ Crystals

927J0005F Leningrad FIZIKA TVERDOGO TELA in Russian Vol 33 No 1, Jan 91 pp 104-109

[Article by Yu.V. Ilisavskiy, V.M. Sternin, R.A. Suleymanov, F.M. Salayev, and M.Yu. Seidov, Institute of Physics at AzSSR Academy of Sciences, Baku]

UDC 537.226:536.42

[Abstract] An experimental study of phase transitions in multilayer $TlInS_2$ and $TlGeS_2$ semiconductor crystals was made by the ultrasonic method, for the purpose of verifying the transition to an incommensurate phase and the subsequent transition to a commensurate phase with attendant quadrupling of the lattice period along the c-axis. Tests were performed with 30 MHz ultrasonic waves propagating through a crystal parallel to its layers, these waves being plain or polarized normally to the stack, and with 30 MHz ultrasonic wave propagating across the stack of layers. Both velocity and attenuation of these waves were measured at temperatures covering the 300-80 K range at a rate of 0.3-0.5 K, the velocity by superposition of echo pulses and the attenuation on the basis of their logarithmic amplitude decrement. Considering that crystals of both semiconductor materials have a nearly tetragonal structure at room temperature, the peaks characterizing the temperature dependence of both wave propagation parameters for all three types of ultrasonic waves in these crystals confirm that transition to a commensurate phase takes place in two stages through an incommensurate intermediate phase as the temperature is lowered. An additional phase transition may, moreover, be taking place in $TlInS_2$ crystals within that intermediate stage. Figures 2; references 23.

Molecular-Beam Epitaxy of GaAs on Hydrogen-Impregnated Si(001) Surface

927J0013B Leningrad PISMA V ZHURNAL TEKHNICHESKOY FIZIKI in Russian Vol 17 No 2, 26 Jan 91 pp 19-23

[Article by V. G. Antipov, S. A. Nikishin, and D. V. Sinyavskiy]

[Abstract] An experiment involving molecular-beam epitaxy of GaAs on Si substrates was performed with a lower than conventional 750° preheat of the substrates but with a chemical pretreatment ensuring formation of the SiH_2 phase on their surface. The substrates, standard Si wafers with [100]+/-20' orientation were chemically pretreated as follows: washed with toluene and acetone—oxidized in boiling HNO_3—etched with HF—repeatedly immersed in aqueous $HCl+H_2O_2$ solution for formation of a thin oxide layer and washed with water after each immersion. The substrates were then transferred, on a molybdenum tray, into the storage chamber of an EP-1301 molecular-beam apparatus and held there under a vacuum of 70 nPa maximum. Their surface structure was examined in the analytical chamber of this apparatus, by Auger-electron spectroscopy and by low-energy electron diffraction using a four-grid electroanalyzer with reverse scan of the diffraction pattern. The diffractograms revealed a (1x1) structure of the Si(001) substrates after treatment with HF in ethanol, indicating presence of the SiH_2 phase. The intensity of oxygen Auger-signals (510 eV) was below the spectrometer noise level, indicating absence of an oxide phase. The intensity ratio of carbon Auger-signals (272 eV) to silicon Auger-signals (92 eV) was within the 10^{-5} - 10^{-5} and thus not larger than permissible after conventional 750°C preheat of Si substrates. Epitaxial growth of amorphous GaAs layers was effected by two methods: 1) substrate heated

to about 200°C and held at this temperature for up to an hour—substrate cooled to about 100°C—continuous 20-30 nm thick GaAs layer grown at a rate of about 0.10 μm/h with a $J_{As4}/J_{Ga} \approx 20$-30 ratio of vapors—substrate with GaAs layer heated to about 620°C and held at this temperature in an As_4 vapor stream of $J_{As4} = (1.5\text{-}3.5) \times 10^{15}$ atoms/(cm^2.s) intensity—GaAs layer further grown at a rate of about 1 μm/h for 3-3.5 h with a $J_{As4}/J_{Ga} \approx 2$ ratio of vapors—substrate with GaAs layer cooled to room temperature; 2) substrate annealed at 500-550°C in growth chamber of the EP 1301 molecular beam apparatus under an As_4 background pressure not higher than 1 μPa—GaAs layer grown at a rate of about 0.2 μm/h for up to an hour with a $J_{As4}/J_{Ga} \approx 15$-25 ratio of vapors—substrate with GaAs layer annealed at about 620°C—substrate cooled to 450-300°C—GaAs layer further grown to a thickness of 1.6-1.8 μm with a $J_{As4}/J_{Ga} \approx 1.5$ ratio of vapors—GaAs layer annealed at about 620°C in an As_4 vapor stream of 2×10^{15} atoms/(cm^2.s) intensity—GaAs layer further grown at a rate of about 1 μm/h at 580-600°C for 2.5 h with a $J_{As4}/J_{Ga} = 1.5$-2 ratio of vapors substrate with GaAs layer cooled to room temperature. In the first case, reflection high-energy electron diffraction (RHEED) revealed a retention of the Si(1x1) surface structure during treatment at 200°C to 100°C and a Si(2x2) surface structure with a "lemon rind" texture after subsequent treatment at 600-630°C. In the second case, Auger-electron spectroscopy and low-energy electron diffraction as well as reflection high-energy electron diffraction revealed a Si(1x1) → Si(2x1) + Si(1x2) structural transformation of the substrate surface owing to hydrogen desorption with attendant As adsorption during treatment at 500-550°C and then a Si(4x4) → Si(2x2) structural transformation of the substrate surface during cooling to room temperature after subsequent treatment at 580-620°C. The authors thank V. Ye. Umanskiy and S. N. Mikhaylov for helpful discussions. Figures 2; references 10.

Epitaxial GaAs Layers With Background Acceptor Impurity

927J0013C Leningrad PISMA V ZHURNAL TEKHNICHESKOY FIZIKI in Russian Vol 17 No 2, 26 Jan 91 pp 28-32

[Article by T. V. Yesipova, Yu. V. Zhilyayev, A. G. Kechek, N. I. Kuznetsov, G. R. Markaryan, and M. G. Mynbayeva, Institute of Engineering Physics imeni A. F. Ioffe, USSR Academy of Sciences, Leningrad]

[Abstract] An experimental study of epitaxial GaAs layers grown in a chloride system was made, those grown on n$^+$-substrates having been doped with Sn or Te and those grown on p$^+$-substrates having been doped with Zn. The substrates had been first polished by gas etching to a depth of several microns, before epitaxial GaAs layers were grown on them without doping under an $AsCl_3$ pressure varied over the 0.001-0.01 atm range at a temperature varied over the 690-745°C range. Some amount of $AsCl_3$ was injected into the substrates, one tenth to one fifth as much as was passed over the source at 800-820°C, so as to minimize the activity chloride forming impurities in the GaAs layers. Special measures were taken to attenuate hydrogen pressure fluctuations. Deep centers in such epitaxial GaAs layers were studied by methods of deep-level transient spectroscopy (DLTS). During spectroscopy in the constant-capacitance mode, the width of the depletion layer remained constant and insensitive to temperature changes. During spectroscopy in the current mode, the width of the depletion layer was changing appreciably and this gave rise to a systematic error. Data have thus been obtained on the ionization energy and the cross-section for capture of charge carriers. Only the pure GaAs layers grown on p$^+$-substrates contained deep H6 acceptors besides deep H2 acceptors, the concentration of the latter increasing depthwise across a layer toward the substrate. Thin layers on these substrates had a p-type conductivity, an i-layer beginning to grow when the thickness had exceeded 25 μ. There were found to be two kinds of GaAs layers grown on n$^+$-substrates: layers containing deep H0, H7, H1 acceptors and layers not containing these acceptors. Layers of the second kind were found to contain deep H2, H3, H4 acceptors and deep E4 donor. The low-temperature photoluminescence spectra of all GaAs layers on n$^+$ substrates recorded at 4 K and their donor photoexcitation spectra obtained by photoelectric laser magnetospectroscopy were analogous to the spectra of such layers grown on i-substrates, the concentration of shallow donors being higher than that of shallow acceptors but neither exceeding 10^{14} cm^{-3}. The high-frequency capacitance of layers with deep H0, H7, and H1 acceptors did not depend on the frequency of the probing signal at temperatures above 150-170 K and became dependent on that frequency at temperatures below 150-170 K. Their capacitance-voltage characteristic at room temperature indicated an about 10^{15} cm^{-3} concentration of ionized impurity and an almost linear dependence of $1/C^2$ on the inverse voltage. While the maximum concentrations of "shallower" H0, H7, and H1 acceptors were each about 10^{14} cm^{-3} each, the combined concentration of deep H0, H7, and H1 acceptors was about 10^{15} cm^{-3}. These layers had accordingly a p-type conductivity. The high-frequency capacitance of layers with deep H2, H3, H4 acceptors and deep E4 donor was frequency-dependent at all temperatures and their base region became semi-insulating at room temperature already. Spectroscopy of these layers had, therefore, to be performed in the current mode only. It was performed with forward charge injecting current pulses and with voltage (inverse) canceling current pulses. These layers were found to have a ν-type or π-type conductivity depending on whether respectively the total concentration of deep donors or deep was higher. Figures 1; tables 1; references 11.

Anomalies of Herschel Effect During Simultaneous Irradiation at Two Different Wavelengths

917J0126A Kiev UKRAINSKIY FIZICHESKIY ZHURNAL Vol 36 No 4, Apr 91 pp 627-629

[Article by M. V. Kurik, Cherkassk Pedagogical Institute, and B. T. Piven, Institute of Physics, UkSSR Academy of Sciences, Kiev]

UDC 77.01.54

[Abstract] A study of the Herschel effect in an actinic photosensitive layer exposed simultaneously to 440 nm radiation and 850 nm radiation was made, in search of an explanation for the much greater strength of this effect during simultaneous irradiation than during sequential irradiation by these different light sources. In the experiment SP-1 layers having a photosensitivity of six units and not forming a latent image when exposed to 850 nm radiation were exposed to both blue light and infrared light, with the energy density of blue light passing through an optical wedge varied and the energy density infrared light not passing through an optical wedge held constant at $E_{850} = 81{,}600 \times 10^4$ erg/cm^2. The layers were then examined under a "Tesla" BS-613 electron microscope (made in Czechoslovakia) with a 0.45 nm resolution. The results indicate that the magnitude of the Herschel effect depends not on the sum but on the ratio of the two radiation intensities, a normal Herschel effect produced by infrared radiation being known to require 10^5 quanta of "erasing" red light per one quantum of blue light. When the ratio was increased to 1578, many fine centers had formed and some of them had combined into a few coagulation centers. When the ratio was increased to 2279.3, more coagulation centers had formed and fewer fine centers had correspondingly remained. When the ratio was increased to 5589.1, smaller fine centers had formed and the coagulation centers had become larger. The number of fine silver particles continued to decrease until that ratio was increased to 9488.4, fine silver particles then having completely disappeared and the amorphous silver coagulation centers having transformed into crystalline latent image centers of developable size on the surface of AgBr microcrystals. Such a transformation from amorphous to crystalline state is consistent with known patterns of electron diffraction by individual Ag-centers. The authors thank V. K. Miloslavskiy for helpful comments on the results of this study. Figures 1; references 7.

On Propane-Air Mixture Detonation Excitation Mechanics in Focused High-Power CO_2 Laser Beam

917J0131C Leningrad PISMA V ZHURNAL TEKHNICHESKOY FIZIKI in Russian Vol 17 No 11, Jun 91 pp 25-29

[Article by G. I. Kozlov, V. A. Kuznetsov, A. D. Sokurenko, Mechanics Problems Institute at the USSR Academy of Sciences, Moscow]

[Abstract] The use of laser radiation on flammable mixtures in order to control the combustion, explosion, and detonation process is discussed and an attempt to initiate detonation of propane-and-air mixtures in a focused laser beam is reported. The experiments were conducted in a quartz tube filled with the mixture under study while radiation of a continuous wave CO_2 laser was injected through a window transparent to laser radiation through one end and was focused at the opposite sealed off end. The latter represents a valve which operated when the pressure in the tube rose above the atmospheric level. The experiment design is described in detail. The experiment revealed that laser radiation initiates an explosion in a mixture already ignited by a spark plug and causes detonation ever without preliminary spark ignition. In order to explain the phenomenon, the process was numerically simulated. An analysis of the results demonstrates that detonation in propane-and-air mixtures in the focused laser radiation field is initiated due to the dissociation of propane molecules in the laser beam and the formation of nonuniform temperature and concentration fields along the channel length in the field, as a result of which gas dynamic processes accompanied by shock and detonation waves are developed. The authors are grateful to S. V. Zakharov for conducting numerical calculations and useful discussions. References 4; figures 3.

Chaotic and Regular Gas Laser Pulse Train Instabilities Given Active Mode Locking Breakdown

917J0132A Moscow KVANTOVAYA ELEKTRONIKA in Russian Vol 18 No 4 (226), Apr 91 pp 405-409

[Article by L. A. Melnikov, G. N. Tatarkov, Scientific Research Institute of Mechanics and Physics at the Saratov State University imeni N. G. Chernyshevskiy]

UDC 621.373.826.038.823

[Abstract] The mode locking operation of lasers emitting trains of short or ultrashort light pulses is addressed; in so doing, special attention is focused on active mode locking (ASM). The formation conditions of the active mode locking operation in gas lasers with inhomogeneous gain line broadening are examined by numerical simulation methods and it is shown that an active mode locking breakdown which is equivalent to changes in the loss modulation frequency lead to the development of regular and chaotic pulse train radiation instability manifested in periodic or chaotic changes in pulse parameters, e.g., energy and duration. The characteristics of the resulting self-excited oscillations are investigated. Equations of the laser's dynamic model are derived allowing for the trapping of resonance emission from the upper working level. It is shown that the appearance of pulse parameter modulation is determined by the patterns of (coherent) nonlinear field interaction with the medium and the ratio between the resonator transmission time

and population difference relaxation time. References 11: 7 Russian, 4 Western; figures 5.

Transient Inversion Grating Generation With Ultrasmall Period in Media With Phase Memory Under Multipulse Interaction

917J0132B Moscow KVANTOVAYA ELEKTRONIKA in Russian Vol 18 No 4 (226), Apr 91 pp 447-451

[Article by S. A. Moiseyev, Ye. I. Shtyrkov, Engineering Physics Institute at the Kazan Scientific Center of the USSR Academy of Sciences]

UDC 621.373.826

[Abstract] Generation of dynamic and spatially periodic structures with a small period in condensed media, particularly by exciting the medium with a standing electromagnetic wave, is considered and the effect of the standing light wave on a medium with phase memory is examined and the shortcomings of standing wave excitation are addressed. To this end, a method of forming inverse gratings with a small spatial period (spacing) which is free of these shortcomings and is based on exciting the medium by alternating pulsed fields which, in contrast to standing wave pumping, do not overlap in a medium with a phase memory is proposed. In so doing, multipulse resonant medium excitation by counterpropagating laser fields is investigated and it is demonstrated that one stable long-lived grating with a supersmall period, i.e., a period which is much smaller than the exciting laser radiation wavelength, may be generated in this medium. Light's interaction with such gratings is analyzed and transient signal generation by such gratings is examined. A technique is proposed for reading data from such gratings; it is shown that this can be effectively used for examining in detail the spectroscopy parameters of atomic systems, relaxation processes, and excitation diffusion at low velocities. References 5: 4 Russian, 1 Western; figures 2.

Electromagnetic Field Generation During Electron Emission Into Outer Gas and Plasma From Disperse Particle Surface Irradiated by Laser

917J0132C Moscow KVANTOVAYA ELEKTRONIKA in Russian Vol 18 No 4 (226), Apr 91 pp 473-478

[Article by V. I. Igoshin, R. R. Letfullin, Samara Branch of the Physics Institute imeni P. N. Lebedev at the USSR Academy of Sciences]

UDC 621.373.826:533.9

[Abstract] The complex of physical processes which develop during the interaction of laser radiation (LI) with condensed disperse phases as a result of which the particles acquire electric potential with a static field in the ambient space is analyzed and the change in the particle's emission parameters in the domain of time which may lead to spontaneous electric and magnetic field generation (GEMP) in the gaseous disperse medium is addressed. The mechanism of electrostatic and quasistatic electromagnetic field generation in gaseous disperse media under the effect of laser radiation within a broad range of particle sizes and laser radiation intensities is proposed and theoretically examined for the first time. Field generation during the electron emission into the ambient gas and plasma around the particle as well as the effect of the particle environment, disperse particle shape, and gas dynamic expansion conditions of the evaporated matter on the particle's potential and emissivity are studied on the basis of feasible physical assumptions. It is shown that effects related to the shape of real disperse particles and electron emission nonuniformity play a dominant role in this process. The results of analytical calculations are quantitatively and qualitatively consistent with experimental data which confirm that thermal electron emission under the effect of laser irradiation may stimulate electromagnetic pulse generation in the RF band whereby the total dipole and quadrupole moments of the charge system play a dominant role. References 21; figures 4.

Optical Breakdown in Aerodisperse Flow

917J0132D Moscow KVANTOVAYA ELEKTRONIKA in Russian Vol 18 No 4 (226), Apr 91 pp 483-485

[Article by P. I. Golubnichiy, V. M. Gromenko, V. G. Shemanin, G. S. Shugurov, Soyuzstromekologiya Scientific Production Association, Novorossiysk]

UDC 621.373.826

[Abstract] Optical breakdown (OP) phenomena in aerodisperse flows are examined from the viewpoint of identifying the origin of optical discharges accompanying high-power laser radiation propagation in the atmosphere under heavy aerosol contamination conditions. The dependence of the threshold energy density, breakdown probability, transmission, and optical breakdown plasma glow intensity on the particle concentration in an air flow with a cement aerosol is examined experimentally. Experimental data are consistent with analytical estimates made on the basis of the theory of low-threshold collective optical discharge and may be used to determine the parameters of optical breakdown in a high-power laser radiation field. The study was carried out in the particle concentration range of 10-1,000 cm^{-3} while neutral light filters calibrated by the IMO-2M power meter were used to measure the laser radiation power. References 7: 6 Russian, 1 Western; figures 4.

Investigation of Plasma-Forming Target Composition of Laser Deuteron Sources for Compact Accelerating Tubes

917J0132E Moscow KVANTOVAYA ELEKTRONIKA in Russian Vol 18 No 4 (226), Apr 91 pp 485-489

[Article by V. M. Gulko, N. F. Kolomiyets, A. Ye. Shikanov, K. I. Yakovlev, Nuclear Research Institute at

the Ukrainian Academy of Sciences, Kiev, and Ramenskoye Branch of the All-Union Science Research Institute of Geological Information Systems]

UDC 621.373.826:533.9

[Abstract] Laser plasma deuteron sources intended for use in pulsed neutron generators and their applications in neutron generating accelerating tubes (UT) are considered. Emissive characteristics of laser deuteron sources as a function of the plasma-forming target material and its stoichiometric ratio are investigated experimentally. The resulting data make it possible to speculate that deuteron emission from laser plasma formed on the surface of deuterides under study tends to increase with the atomic mass of the carrier metal. It is shown that the maximum number of deuterons per deuterium atom corresponds to erbium given a stoichiometric ratio of 1.3. The results point to the expediency of using sealed off accelerating tubes with a laser deuteron source of ErD plasma-forming targets making it possible to increase the neutron yield by almost 2-fold while preserving the accelerating tube's energy supply. References 4; figures 1; tables 1.

New Laser Resonator Mirror

917J0132F Moscow KVANTOVAYA ELEKTRONIKA in Russian Vol 18 No 4 (226), Apr 91 pp 493-494

[Article by A. V. Yurkin, General Physics Institute at the USSR Academy of Sciences, Moscow]

UDC 621.373.826:681.7.062

[Abstract] The parallel arrangement of planar laser resonator mirrors which require accurate alignment is discussed. A simple design of laser resonator mirror consisting of several reflecting planes which are not parallel to each other and are formed by the surfaces of sloping plates or wedges is proposed. Such a mirror makes it possible to obtain a smooth laser beam intensity distribution which is uniform in the beam cross section in a single spot. The results of mirror applications as the output mirror of a solid state laser are described. The use of a laser equipped with such a mirror made it possible experimentally to investigate light-acoustic pulses since it eliminated sound pulses from hot local spots in the intensity distribution both when stimulating light-sound pulses in the bulk of the medium and affecting a light-absorbing surface as well as in other cases which call for producing a uniform rather than jagged sonic or shock pulse. The laser beam energy was equal to 300 J and its beam divergence was $\gamma = 4'$. References 3; figures 3.

Linear Intracavity Laser Spectroscopy With Analytical Frequency Signal

917J0132G Moscow KVANTOVAYA ELEKTRONIKA in Russian Vol 18 No 4 (226), Apr 91 pp 509-514

[Article by A. A. Zheltukhin, I. P. Konovalov, Ye. D. Protsenko, State Scientific Research and Design Institute of Nitrogen Industry and Organic Synthesis Products, Moscow]

UDC 535.374:621.373.826

[Abstract] The use of spectral analysis to detect trace amounts of impurities prompted by environmental concerns and the needs to produce pure substances is discussed. An attempt is made to develop intracavity laser spectroscopy with frequency detection for analytical applications by using the effect of the unsaturated spectral line dispersion on the stimulated mode frequency. To this end, a new method of analytical laser spectroscopy is proposed on the basis of linear repulsion of frequencies of a two-mode dye laser with an internal absorbing cell. The method is illustrated by an experiment in which sensitivity of near 10^9 Hz/cm^{-1} was attained, which is lower than the absolute theoretical limit by less than 10-fold. This sensitivity is found to be independent from the steady-state stimulated emission intensity and duration. The method is comparable to laser fluorescent atomic spectroscopy whose reputation for detecting hertz-like mode shifts is commonly acknowledged; moreover, the method's insensitivity to the field strength lends it for use in lasers with intracavity second harmonic generation (GVG), i.e., extending its spectral range to the ultraviolet (UF) band. References 8; figures 6.

Transformation of Laser Signal Polarization During Passage Through Thermodynamically Irreversibly Crystallizing Water Aerosol

927J0004A DOKLADY AKADEMII NAUK SSSR in Russian Vol 318 No 4, Jun 91 pp 895-897

[Article by L. G. Kachurin and B. Kh. Petkov, Leningrad Institute of Hydrometeorology]

[Abstract] An experimental study was made concerning passage of a linearly polarized laser signal through a thermodynamically irreversibly crystallizing water aerosol and the attendant transformation of its polarization, the transformation of its polarization into an elliptical being in this case determined not only by the crystallization rate, as during passage through a water layer, but also on the orientation of the signal relative to the crystallization front of each aerosol particle. The amplitude-frequency characteristic of polarization transformation, the principal source of information about this phenomenon, was measured with the aid of oscillograms recorded with a photodetector in a fog chamber at temperatures from -5°C to -60°C. Fog was generated by

injection of jets of supersaturated water vapor, in various precisely controlled amounts. Both amplitude of the laser signal and frequency of its amplitude modulation were averaged over the crystallization period, the low-frequency part of the optical spectrum associated with turbulence of aerosol formation in the vapor jet then being excluded from analysis of the spectra. The temperature dependence of the signal amplitude and of its modulation frequency indicates passage of a signal either through a zone where injected vapor first condenses and the condensate then crystallizes or through a zone where injected vapor immediately converts into ice, a depolarizing medium. The probability of predominantly irreversible rather than reversible vapor-to-water transition and subsequent crystallization of water increases with lowering of the temperature, as indicated by an increasing modulation factor and a rising modulation frequency. As the temperature is further lowered, the probability of irreversible direct vapor-to-ice transition increases while the probability of crystallization decreases and the intensity of polarization transformation correspondingly decreases. Article was presented by Academician K. Ya. Kondratyev on 2 March 1991. Figures 2; references 2.

X-Ray Laser With Excitation by Oscillating Electrons in Field of Ultrabright Pumping Laser Beam

927J0006D Moscow IZVESTIYA AKADEMII NAUK SSSR: SERIYA FIZICHESKAYA in Russian Vol 55 No 4, Apr 91 pp 811-817

[Article by I. N. Knyazev, V. V. Korobkin, and M. Yu. Romanovskiy, Institute of General Physics, USSR Academy of Sciences

UDC 533.8

[Abstract] A new type of x-ray laser is proposed, one with a cold gaseous plasma as active medium where free electrons will excite ions and then recombine with them. In such a medium the pump energy should affect only the useful parts of the electron, ion, and plasma radiation emission spectra, which will not only increase the efficiency of such a laser but also narrow its emission band. This is shown to be achieved by direct above-threshold excitation of ions with oscillating electrons, such electrons becoming available when ultrabright ($I > 10^{17}$ W/cm^2) laser radiation has been injected into such a medium. Considering that only the Lorentz force and the Coulomb force act here on a free electron, the process is analyzed by first calculating the frequency of stimulated electron-ion collisions and the velocity of an electron at the instant of collision. The velocity distribution of electrons at the instant of collisions here is certainly a non-Maxwellian one with hot electrons absent so that the spectrum after complete ionization will, advantageously, contain only one ion presumably much heavier than an electron and therefore practically at rest. The total ionization time is calculated next, considering that the electron concentration varies as a function time depending on the rates of impact ionization and Auger ionization. Inasmuch as the ionization stage in a two-laser scheme coincides with the heating stage, a "hole" laser is realizable only prior to complete ionization while only conventional Ne-like or Ni-like schemes with direct impact excitation after complete ionization but also with adjustable pump pulse duration are feasible. A scheme with recombination during a pump pulse is not feasible, inasmuch as the speed of recombination even to upper levels in a dense gaseous medium is much lower than the characteristic speed of processes occurring in the active medium of an x-ray laser. A scheme with recombination after a pump pulse is feasible, as it is in conventional schemes. Because the detailed balance principle does not apply here, the speed of recombination must be determined directly as the product of two probabilities: probability of electron-ion collision in units of time after which an electron will "stick" to an ion and least probability of another electron being near the ion so that excess energy of the forming system will be diverted to it. Following this analysis, the three possible schemes are each evaluated in terms of requirements for and small-signal performance of x-ray lasers. The scheme with "hole" lasing during internal ionization offers realizability of the $2 \rightarrow 1$ transition to the ground state and consequently maximum efficiency, only this scheme being feasible with pump pulses shorter than the total ionization time. This scheme and the scheme with direct impact excitation, of an Ne-like (Se) or Ni-like (Eu) laser, are feasible with pump pulses longer than the total ionization time and operates from after the end of a pump pulse till complete ionization. The recombination scheme, feasible with pump pulses shorter than the plasma formation time, operates from after the end of a pump pulse till plasma formation and its subsequent heating. With this scheme, however, the density of the medium must be limited and the x-ray emission level will be limited, as demonstrated on an Ne-like (Se) laser. Nevertheless, H-like, He-like, and Li-like recombination lasers are apparently quite feasible. Figures 4; references 5.

Semiconductor Power Laser Arrays Produced by Molecular-Beam Epitaxy

927J0009C Leningrad PISMA V ZHURNAL TEKHNICHESKOY FIZIKI in Russian Vol 17 No 7, 12 Apr 91 pp 31-34

[Article by S. Yu. Karpov, H. de la Cruz, V. Ye. Myachin, A. Yu. Ostrovskiy, Yu. V. Pogorelskiy, I. Yu. Rusanovich, I. A. Sokolov, N. A. Strugov, A. L. Ter-Martirosyan, G. A. Fokin, V. P. Chelyy, A. P. Shkurko, and M. I. Etinberg, Institute of Engineering Physics imeni A. F. Ioffe, USSR Academy of Sciences , Leningrad]

[Abstract] Semiconductor laser arrays built on AlAs-GaAs solid solutions were experimentally produced by molecular-beam epitaxy, as model heterostructure optimizable in terms of maximum emission power with a

sufficiently high differential quantum efficiency having been selected one on an n-GaAs:Sn ($n \approx 8 \times 10^{17}$ cm^{-3}) substrate with a GaAs quantum well as active region. On top of such a substrate, separated from it by 0.8 μm thick n-GaAs:Si ($n \approx 6 \times 10^{17}$ cm^{-3}) buffer layer, was deposited a symmetric five-layer structure: a 2.2 μm thick n-$Al_{0.42}Ga_{0.58}As$:Si ($n \approx 6 \times 10^{17}$ cm^{-3}) wideband n-emitter, an 80 nm thick n-$Al_{0.23}Ga_{0.77}As$:Si ($n \approx 6 \times 10^{17}$ cm^{-3}) waveguide, a 15 nm thick GaAs ($n \approx 1 \times 10^{15}$ cm^{-3}) active medium, an 80 nm thick identical waveguide, and a 2.2 μm thick Be:p ($p \approx 3 \times 10^{17}$ cm^{-3} wideband p-emitter). These structures were experimentally evaluated, the test results indicating that $Al_xGa_{1-x}As$ layers with $x = 0.20$-0.45 suitable for laser devices are attainable by vapor deposition of an As_4:(Al + Ga) ≈ 2 mixture at a temperature correspondingly within the 610-640°C range but with $n < 10^{17}$ in the buffer layer so as to avoid Si segregation on the surface. Control specimens of cloverleaf laser diodes were then built from such structures, the threshold current density for light emission being 250-300 A/cm^2 regardless of their size. Also mesa lasers in the form of a 100 or 200 μm wide strip with additional oxide insulation were built, the threshold current density for those in a 1.2 mm long optical cavity being 300 A/cm^2. The differential quantum efficiency of the short-strip lasers reached 75-80 percent regardless of the strip width and the emission power of individual 100 μm wide strip lasers reached 800-900 mW without additional coating. Such lasers were subsequently assembled into arrays of 10-15, with 100 μm wide clearances between 100 μm wide strips. On the back mirror of each array was deposited a multilayer metal-dielectric ensuring an 80 percent reflectance. They were tested in quasi-continuous operation at room temperature (15°C), pumped with electric current in pulses of 200 μs duration at a repetition rate of 50 Hz. Figures 2; references 8.

Picosecond Relaxation Processes in Semiconductor Laser Pumped by Ultrashort Pulses of High-Intensity Ultraviolet Light

927J0016B Moscow ZHURNAL EKSPERIMENTALNOY I TEORETICHESKOY FIZIKI in Russian Vol 99 No 6, Jun 91 pp 1793-1803

[Article by Yu. D. Kalafati and V. A. Kokin, Institute Radio Engineering and Electronics, USSR Academy of Sciences]

[Abstract] A theory of relaxation processes in a semiconductor laser pumped by ultrashort pulses of high-intensity ultraviolet light is developed on the basis of equations describing the dynamics of electron-hole plasma behavior and of stimulated radiation emission during intense heating of excess charge carriers. These two equations, of plasma energy balance and electron concentration balance respectively, are formulated in the quasi-equilibrium state approximation. This is permissible, inasmuch as the temperature of electrons and the temperature of holes in an electron-hole plasma with an electron concentration $n > 10^{17}$ cm^3 in a semiconductor are known to become equal within a time shorter than 1 ps. An analytical solution of these equations is possible when the evolution of stimulated processes passes through three successive stages with widely different time scales, as it does in a semiconductor such as GaAs. They are solved accordingly, by the method of small-parameter perturbations with the ratio of the mean photon life τ_{ph} in an optical cavity to the characteristic plasma cooling time t_T as the small parameter. In the "ultrafast" first stage there occurs no significant temperature change, the time scales here being τ_{ph} (mean photon life in optical cavity) and $1/G_{max}c$ (G_{max} - maximum gain, c - speed of light in semiconductor). In the "fast" second stage which follows there occurs a change of plasma temperature, the time scales here being the characteristic electron energy relaxation time τ_e and hole energy relaxation time τ_h. In the "slow" third and last stage there occurs stimulated recombination with attendant radiation damping, the time scales here being much larger than the characteristic plasma cooling time. In accordance with this theory is considered excitation of a GaAs semiconductor laser by picosecond ultrashort pulses of high-intensity ultraviolet light, also by subpicosecond pulses of such a light. The authors thank I. L. Bronev, S. Ye. Kumekov, and V. I. Perel for helpful discussion of the results, also G. N. Shkerdin, and Yu. V. Gulyayev for interest and support. References 25.

Thermal Physics of Cooled Laser Mirrors

927J0030A Moscow TEPLOFIZIKA VYSOKIKH TEMPERATUR in Russian Vol 29 No 2, Mar-Apr 91 pp 365-375

[Article by V. I. Subbotin, V. V. Kharitonov, Moscow Engineering Physics Institute]

UDC 621.039:536.24

[Abstract] The problem of thermal physics of mirrors—an integral part of lasers—which must meet very stringent requirements imposed on the surface finish of the reflecting surface, low laser radiation absorption, stability of the geometrical and physical parameters during operation, etc., is discussed. A precise solution of the spatial problem of thermoelasticity of laser disc mirrors is cited and today's status of the theory of turbulent mass transfer in systems of cooled mirrors is briefly reviewed. Two-temperature equations of convective heat transfer in laser mirrors are derived in the porous body approximation and the universal relationship of convective heat transfer and the friction pressure loss of porous media is established. Turbulent heat conduction of liquids in porous media is investigated and the limits of heat transfer enhancement in mirrors are determined. Two-dimensional effects of localized heating in a multilayered target with a cooled porous layer are examined and the effect of convective heat transfer on the transient straining of mirrors is analyzed. It is shown that improvements in the model of an anisotropic porous medium will make it possible to extend it to analyzing

thermal hydraulic processes in diverse physical power plants. Figures 8; references 27.

Evaporation of Drop in Optical Radiation Field

927J0040B Moscow TEPLOFIZIKA VYSOKIKH TEMPERATUR in Russian Vol 29 No 3, May-Jun 91 pp 577-581

[Article by S. A. Beresnev, V. G. Chernyak, Urals State University]

UDC 533.72+541.182

[Abstract] Evaporation kinetics of drops in an optical radiation field and the related aerodisperse medium phototropism under the effect of laser radiation are discussed. An attempt is made to formulate a molecular kinetic description of the evaporation of drops of an arbitrary shape suspended in the atmosphere of their own vapors under the effect of unilateral electromagnetic radiation. The problem is solved in a quasisteady approximation on the basis of a linearized gas kinetic equation within the entire range of Knudsen Kn numbers allowing for the thermal, accommodation, and optical properties of the drop. The problem is formulated as a spherical particle suspended in a medium of its own equilibrium vapor upon which uniform radiation is incident along the *OZ*-axis. The following simplifying assumptions are made: the radiation does not interact with the vapor but only with the drop substance while absorption is described by Mie's macroscopic theory; the effect of the drop's surface curvature on the saturated vapor pressure may be ignored; and the drop surface temperature differs very little from the vapor's equilibrium temperature. In contrast with the local molecules' flux, the integrated flux of evaporated molecules does not depend on the particle heat conduction. It is shown that experiments with drop evaporation in the laser radiation field may, in principle, provide information about the accommodation and optical properties of submicrometer particles. Figures 1; references 5: 4 Russian, 1 Western.

New Solution to Equations of Magnetohydrodynamics

927J0013E Leningrad PISMA V ZHURNAL TEKHNICHESKOY FIZIKI in Russian Vol 17 No 2, 26 Jan 91 pp 70-72

[Article by A. T. Skvortsov, Institute of Acoustics imeni A. N. Andreyev, USSR Academy of Sciences, Moscow]

[Abstract] A new approach is taken to the problem of solving the Graede-Shafronov equation of magnetohydrodynamics $\Delta\Psi = r^2P'-ff'$ for the axisymmetric equilibrium configuration of an ideally conducting liquid, where Ψ is Stokes' potential and ($\Delta = \delta^2/\delta z^2 + (r\delta/\delta r)(\delta/r\delta r)$ in cylindrical coordinates r,z,θ (f - arbitrary function). Upon letting $f = k\Psi$ and $P = m^2\Psi^2 + d$ (k,m,d - constants), its solution is sought in the form $\Psi = Z(z)R(r)$. Insertion of Ψ in this form reduces that equation to the equality $-Z''/z = (R''-R'/r)/R + k - m^2r^2$. This equality can be satisfied only when the comparable quantities are equal to a constant and, for a finite solution at $z \to \infty$, to a positive one. Letting this constant be q^2 will then lead to two equations: $z'' + q^2Z = 0$ with the trivial solution $Z = A\cos(qz) + B\sin(z)$ (A,B-constants) and $R''-R'/r+ (k^2 - q^2 - m^2r^2)R = 0$ reducible to a hypergeometric one by letting $mr^2 = \xi$ so that its solution will be a degenerate hypergeometric function reducible to canonical form. The exact solution to the original equation thus describes a magnetic field distribution with an exponential radial (r) profile and a periodic longitudinal (z) profile. Such a solution can also be obtained for vortical axisymmetric flow in plain hydrodynamics. References 5.

Morphology of Solid Solutions in Vicinity of Nonequilibrium Phase Transition Induced by Ion Irradiation

917J0099A POVERKHNOST: FIZIKA, KHIMIYA, MEKHANIKA in Russian No 2, Feb 91 pp 55-60

[Article by V. S. Khmelevskaya, V. G. Malynkin, S. I. Kashirin, and Ye. V. Kudrya]

UDC 539.1.043:669.018.44

[Abstract] Phase transition of several alloys (Fe-Ni, Fe-Cr, Ni-Cr, Ni-Cu, Fe-Ni-Cr solid solutions) induced by ion irradiation (40 keV Ar^+, 1 Mev Ar^+, 50 keV Ni^{2+}) was studied experimentally in an x-ray diffractometer and under an electron microscope. A structural transformation is known to attend thus induced phase transition of solid solutions from one-phase state to a two-phase state. The new structure does not represent proximity to an equilibrium state, however, inasmuch as it is known to break down upon annealing at a temperature not higher than the ion irradiation temperature. Structural transformation attended this phase transition of all alloys alike but different changes indicating it occurred in the diffraction patterns of alloys with f.c.c. crystal lattices and of alloys with b.c.c. crystal lattices. In the diffraction patterns of alloys with f.c.c. crystal lattices (0Cr18Ni10Ti steel) the original peak was replaced by two new peaks corresponding to different lattice periods, indicating that the transition was not at all or at least not only due to concentrational segregation. In the diffraction patterns of Fe-Cr alloys with b.c.c. crystal lattices (Cr12MoVWNb steel) ion irradiation within a certain temperature range had caused the x-ray lines to acquire a cosinusoidal form, indicating a superposition of a sharp Debye peak and a milder neighboring diffusion peak. The attendant anomalous morphological changes have been found to be similar in alloys with both kinds of crystal lattice, three stages of change being distinguishable as the perturbations caused by ion irradiation increased. In the first stage (small ion irradiation doses and low temperatures) the microstructure of the alloys had remained "normal" and included some dislocation loops. In the second stage (larger ion irradiation doses and higher temperatures) the number of dislocation loops was larger, not only dislocation loops forming in various planes but simultaneously dendritic dislocations and striae with "dipole" boundaries. The most numerous element of the microstructure characteristic of this stage were sites with patchy contrast between regions of different illuminance levels, most often turned relative to one another. In the third stage (still larger ion irradiation doses and higher temperatures) the microstructure changed again, now to one corresponding to coexistence of more than one phase and characterized by a cellular defect structure with a dimensional hierarchy of cells. The results of examination under an electron microscope indicate that in the vicinity of such a nonequilibrium phase transition, evidently one consistent with thermodynamics of irreversible processes, the interaction of bombarding ions and alloy leads to development of a specific cellular instability similar to that which develops as a result of irradiation by a plasma beam or a laser beam. Figures 4; references 10.

Potential of Image Forces at Surface of Dielectric Under Metal Coating

917J0099B Moscow POVERKHNOST: FIZIKA KHIMIYA MEKHANIKA in Russian No 2, Feb 91 pp 86-89

[Article by L. G. Ilchenko and L. G. Grechko, Institute of Surface Chemistry, UkSSR Academy of Sciences, Kiev]

UDC 539.2.01

[Abstract] The electrostatic potential energy of a charge in vacuum near the surface of a dielectric substrate under a metallic adsorbate coating is calculated by the method of Green's functions for a longitudinal Coulomb field in media with spatial dispersion, the image forces at the substrate surface being described according to the model of three media: dielectric material with permittivity ε = const occupying region $x < -L$, metal with a Thomas-Fermi permittivity function occupying region $-L \leq x \leq 0$, vacuum in region $x > 0$. From the general expression for the electrostatic energy V(x) of a point charge Z^*e in vacuum near the dielectric under a metal layer of thickness L are obtained asymptotic expressions for the potential of image forces V(x) in this system in the two extreme cases of a metal layer thickness much larger and much smaller than the Thomas-Fermi shielding radius. The effect of metal submonolayer and monolayer coatings on that potential is analyzed on this basis, assuming sufficient surface coverage for formation of a two-dimensional metallic state with charge carriers (electrons or holes) by direct exchange interaction of adatoms and considering a metal film with a dimensionally quantized electronic spectrum in the limiting case of one occupied two-dimensional subband. Metallization of a dielectric substrate is found to strengthen the charge-substrate interaction, already a monolayer metal coat causing the potential of image forces to increase asymptotically in a manner characteristic of atomically pure metal surfaces. References 8.

Kinetics of Surface Layer Formation During Ion-Beam Deposition of Coating

917J0099C Moscow POVERKHNOST: FIZIKA KHIMIYA MEKHANIKA in Russian No 2, Feb 91 pp 90-95

[Article by V. I. Gorokhovskiy, A. G. Zhiglinskiy, V. V. Kuchinskiy, E. N. Fafurina, V. A. Fomichev, and A. S. Shulakov]

UDC 539.26:535.5

[Abstract] Surface hardening by ion-beam deposition of a coating for higher wear resistance and longer tool life is considered, a physical model of mass transfer being proposed for a theoretical description of the kinetics of a two-component coating formation with respective two atom concentration distributions across the transition layer and ultrasoft x-ray emission spectroscopy being proposed for experimental determination of the respective two concentration profiles. This model, more comprehensive than all known ones, includes all diffusion processes associated with action of an ion beam: radiation-stimulated diffusion with cascade mixing and ordinary thermal diffusion. The two respective coefficients D_n and D are lumped into one dimensionless parameter $G = (D_n + D)/Jh^4$ (J - incident ion flux, h - distance between atom layers), the energy of an ion beam being usually so low that surface deposition without deep penetration can be assumed. The general equation for the general time and depth dependent atom concentration of each element (depth in h units) is solved for boundary conditions corresponding to the practical case of a time-independent average atom flux of the deposited element. The equation is solved by Laplace transformation of both sides, application of Borel's theorem, and inverse Laplace transformation. The subsequent numerical solution is not destabilized by variation of the value of D_n, which is not precisely known, within the 5×10^{-14} - 2×10^{-13} cm^2/s range (D = 0). Concentration profiles calculated on this basis for a carbon coating on an aluminum substrate are compared with concentration profiles determined experimentally on the basis of ultrasoft x-ray emission spectroscopy over a 5 min or longer period of time. The conventional version of this method based on action of an electron beam on a solid target and on filling vacancies in inner atom shells, with the embedded depth of an x-ray source depending on the energy of the incident electron beam and on characteristics of the target material such as its density and effective atomic number, has been modified for this application by varying the electron beam energy and thus the probing depth. Independent determinations of concentration profiles were also made on the basis of Auger electron spectroscopy. The results obtained by the two experimental methods are close and agree closely with the results of theoretical calculations, indicating an about (700-800)h thick transition layer. Figures 2; references 6.

Estimated Mean Life of Massive Nuclear-Unstable Fragments of ^{238}U Fission by 1 GeV Protons

917J0127A Moscow PISMA V ZHURNAL EKSPERIMENTALNOY I TEORETICHESKOY FIZIKI in Russian Vol 53 No 8, 25 Apr 91 pp 385-388

[Article by A. V. Kravtsov and G. Ye. Solyakin, Leningrad Institute of Nuclear Physics imeni B. P. Konstantinov, USSR Academy of Sciences, Gatchina]

[Abstract] An experiment was performed involving fission of ^{238}U nuclei by 1 GeV protons and use of a two-arm time-of-flight spectrometer, for a study of the massive nuclear-unstable fission fragments and estimation of their mean life. Measurements were made with the spectrometer arms in a collinear configuration 180° apart and in a noncollinear configuration 170° apart, the stationary arm being always oriented perpendicularly to the primary particle beam. With the other arm in line there were recorded 22,000 fission events and with the other arm 10° off there were recorded 88,000 fission events. From all events were selected those with attendant nucleon losses $\Delta M = A_0 - (M_1 + M_2 \geq 75$ amu), 204 such events having been recorded in the collinear configuration and 444 such events having been recorded in the noncollinear configuration. Only these events were used for plotting the time distributions of events on the basis of the net momentum transferred to two fragments or, more precisely, of its projections $P(t) = P_1(t) - P_2)(t)$ onto the axis perpendicular to the primary particle beam. Both distributions were then processed in an identical manner, assuming each to be the sum of a normal one with a zero mean and a dispersion $\sigma_P = 449$ MeV/s dispersion plus a complementary one. Further calculations are based on the relation $t = gt[(1/2)\log(1 + x)/(1 - x) + x/(1 - x^2)]$ for the time of motion t of two bodies subject to Coulomb attraction ($x = P/P_0$, P - momentum at given instant of time, P_0 - maximum possible momentum acquired by fragment upon its acceleration, $\tau = 2e^2Z_1Z_2\mu^2P_0^{-3}$, $Z_{1,2}$ - charges of fragments, μ - reduced mass of fragments). The experimental data pertaining to collinear and noncollinear configurations respectively fit, after normalization, a system of two equations for the time constant of the fission process $N(t) = N_0e^{-\lambda t}$. With $P_0 = 3000$+/-20 MeV/s and $\lambda = (5.7$+/-0.5) $\times 10^{20}$, the mean life of those fragments is $\lambda^{-1} = (1.8$+/-0.2) $\times 10^{-21}$ s. Figures 3; references 4.

New Analysis of Data From Facility at Moscow State University on Number-of-Particles Spectrum of Extensive Air Showers

927J0006A Moscow IZVESTIYA AKADEMII NAUK SSSR: SERIYA FIZICHESKAYA in Russian Vol 55 No 4, Apr 91 pp 678-681

[Article by V. B. Atrashkevich, O. V. Vedeneyev, G. V. Kulikov, A. A. Silayev, V. I. Solovyeva, V. P. Sulakov, A. V. Trubitsyn, Yu. A. Fomin, and G. B. Khristiansen, Scientific Research Institute of Nuclear Physics at Moscow State University imeni M. V. Lomonosov]

UDC 537.591.15

[Abstract] Data obtained at Moscow State University on extensive air showers have been analyzed anew, the differential number-of-particles spectrum of these showers having been determined on the basis of a modified formula for the space distribution function of charged particles in such a shower rather than on the basis of the old empirical formulas $f(r) = 0.002r^{-1}e^{-r/80}$ (r

$\leq$ 96 m) and $f(r) = 0.6r^{-2.6}$ ($r \geq 96$ m) with altitude above sea level r as argument and the family of Nishimura-Kamata functions with the age parameter s as argument in the Greisen approximation. The new formula for the space distribution function is $f_m(r,s') = [\Gamma(3.9 - s')/2\pi R_0^2\Gamma(s')\Gamma(3.9 - 2s')][(r/R_0)^{s'-2}]$ $[(1 + r/R_0)^{s'-3.9})]$ with $R_0 = 80$ m. Also, taken into account is the fact that, as the number of charged particles N varies, so do the mean values of parameter s' over narrow intervals of N: they decrease as N increases up to 5×10^6 and then increase as N increases further. Figures 2; references 10.

Prototype Deep-Water Neutrino Telescope in Self-Contained Module and Results of Its Field Tests

927J0006B Moscow IZVESTIYA AKADEMII NAUK SSSR: SERIYA FIZICHESKAYA in Russian
Vol 55 No 4, Apr 91 pp 755-757

[Article by A. O. Deyneko, I. M. Zheleznykh, V. A. Zhukov, L. M. Zakharov, A. A. Permyakov, and N. M. Surin, Institute of Nuclear Research at USSR Academy of Sciences, A. P. Yeremeyev, M. Yu. Platonov, and N. A. Sheremet, Institute of Oceanography at USSR Academy of Sciences]

UDC 537.591.8

[Abstract] The authors have designed and built a prototype deep-water neutrino telescope in a self-contained module for detection of cosmic particles, this module having been tested during the 45th voyage (October-December 1989) of the "Dm. Mendeleyev" scientific research ship. The module contains a group of photomultipliers which record Cerenkov radiation and are connected to a common events sampling system, a separate power supply, and a special-purpose primary data processor. The module contains four Hamamatsu-R2018 Vavilov-Cerenkov radiation sensors with hemispherical photocathodes, each inside a spherical transparent glass housing designed for hydrostatic pressures up to 67 MPa, a depth sensor and a spatial orientation sensor inside a common cylindrical titanium alloy housing. The module also contains all electronic components including the primary data processor, inside a spherical metal housing designed for hydrostatic pressures above 60 MPa, and a bank of submersible 12 V storage batteries with 215 A.h capacity each. The module is mounted in a stainless steel frame. As the module reaches a specified depth, it is automatically activated by a signal from the pressure transducer. Pulse signals appearing at the photomultiplier anodes are amplified and then converted into standard paraphase ESL pulses of 40 ns duration for further transmission to a quadruple coincidence circuit with a time resolution equal to the maximum muon time-of-flight through the system. Data put out by the primary processor are stored on a magnetic disk. The overall size of the module is 8x8x8 m^3, it weighs 540 kgf in air and 80 kgf in water. It is submersible to a depth of 6 km and draws a power of 60 W. The authors thank M. A. Markov and V. S. Yastrebov for very stimulating discussions. Figures 2; references 5.

Diffuse Spectra of Ultrahigh-Energy pγ-Neutrinos

927J0006C Moscow IZVESTIYA AKADEMII NAUK SSSR: SERIYA FIZICHESKAYA in Russian
Vol 55 No 4, Apr 91 pp 758-760

[Article by V. S. Berezinskiy and S. I. Grigoryeva, Institute of Nuclear Research at USSR Academy of Sciences, A. Z. Gazizov, Institute of Physics imeni B. I. Stepanov at BSSR Academy of Sciences]

UDC 523:539.123

[Abstract] The diffuse spectra of ultrahigh-energy ($E_\nu \geq$ 1 PeV) pγ-neutrinos have been calculated, such neutrinos being produced principally in collisions of ultrahigh-energy cosmic rays and relict photons. The calculations are based on three assumptions: 1) the universe expands according to the Friedman model with the density of matter equal to the critical one; 2) all cosmic rays have been generated within a z_f = 5-100 epoch during a relatively short ($\Delta z << z_f$) "bright phase of galaxies" burst of massive star formation from collapsing giant objects, with a power-law differential spectrum of these cosmic rays truncated on the high-energy side; 3) a Planckian photon spectrum with the temperature $T_0 = 2.72$ K into the contemporary epoch and a $(1 + z)^3$ times higher photon concentration in a $(1 + z)$ epoch. Inasmuch as the evolution of the proton spectrum is quite intricate, the energy $E_p(E_g,z_f,z)$ was calculated by taking into account all energy losses including those on the red shift, formation of e^+e^--pairs, and production of mesons. The differential spectra of mu-neutrinos have been calculated in this way for $z_f = 5$ and 20, $\gamma_g = 1.1$, 1.3, and 1.5, and an $E_{max} = 10^{10}$ TeV truncation energy of the proton spectrum. Figures 1; references 6.

Covariance Approach to Theory of Photonuclear Reactions $\gamma 0^+$ $1/2^+1/2^+$ and to Their Realization on ^{4}He

927J0007A Moscow YADERNAYA FIZIKA in Russian
Vol 53 No 2, Feb 91 pp 365-390

[Article by S. I. Nagornyy, Yu. A. Kasatkin, V. A. Zolenko, I. K. Kirichenko, and A. A. Zayats, Kharkov Institute of Engineering Physics, UkSSR Academy of Sciences]

[Abstract] A relativistic approach to the theory of photonuclear reactions involving scalar systems is developed which not only satisfies the fundamental requirements of Lorentz gauge invariance, namely covariance and exact gauge invariance without kinematic singularities, but also takes into account internal dynamics of nuclei, rescattering effects, and exchange currents. Two such $\gamma 0^+ \rightarrow 1/2^+1/2^+$ reactions involving a spinless ^{4}He nucleus are considered: $^4He(\gamma,p)^3He$ and $^4He(\gamma,n)^3He$ photofission reactions, their matrix element being determined by

electromagnetic interaction (A_μ) of spinor fields ($\Psi^{(\alpha)}$, α = N,T) and scalar fields (B). The gauge-invariant amplitudes of these reactions and the cross-sections for them are calculated analytically in accordance with a quantum field theory, using expansions of and Ward-Takahashi identities for compendent three-point and four-point Green's functions. Two diagrams of the ^{4}He(γ,N)T reaction with T and N channels in the Coulomb gauge are constructed, also a diagram describing lower-order scalar NN-interaction in the $g\psi^2\varphi$ model and a diagram describing the mesonic exchange current based on "minimal inclusion" of the electromagnetic field in the expression for the reaction amplitude in terms of the compendent four-point at Green's function. Both the ^{4}He $\rightarrow$ NT vertex with a single virtual component and the NT $\rightarrow$ NT vertex are then determined, using available data on the structure of oligonucleonic systems rather than the Bethe-Salpeter equations, whereupon the effect of rescattering in electric dipole E1 transitions is also evaluated. An analysis of numerical data covering the low-energy range, up to 50 MeV, validates this covariance approach to photofission of the ^{4}He nucleus. The results indicate that at the reaction threshold, which is $E_\gamma \approx 22$ MeV, the effect of exchange currents is compensated, also that their role as well as the role of other mechanisms and also the role of interactions in the final state may be overestimated if exact gauge invariance is disregarded in calculations. They further indicate that peaking of the cross-sections for (γ,p) and (γ,n) reactions to their respective maxima at energy levels about 26 MeV is not due to collective excitations of the ^{4}He nucleus from the ground state but due to rescattering in E1 transitions, also that Coulomb effects as well as the difference between the mass of ^{4}He and the mass of ^{3}He cause the cross-sections in the (γ,p) channel to be up to three times larger than those in the (γ,n) channel at the $E_\gamma \approx 22$ MeV reaction threshold. Measurements made under identical conditions confirm the isotopic invariance of strong interactions, the amplitudes of both ^{3}He $\rightarrow$ n + ^{3}He and reverse charge transfer processes in P-waves being evidently small. The covariance approach may be applicable to photofission of other scalar systems such as heavier nuclei (^{12}C, ^{16}O) as well. The authors thank D. V. Volkov and S. V. Peletminskiy for very stimulating discussions of the quantum-field aspects of the problem, also Ye. V. Inopin, P. V. Sorokin, and V. I. Voloshchuk for interest and valuable comments. Figures 10; references 56.

Inclusive Production of K^0-Mesons in K^+A-Interactions at 11.2 GeV Energy Level

927J0007B Moscow YADERNAYA FIZIKA in Russian Vol 53 No 2, Feb 91 pp 429-438]

[Article by S. A. Akimenko, V. I. Belousov, V. N. Kolosov, V. M. Kutin, Yu. M. Melnik, A. I. Pavlinov, A. S. Solovyev, V. V. Churakov, and A. Ye. Yakutin, Institute of High-Energy Physics in Serpukhov, A. M. Artykov, Scientific Research Institute of Applied Physics at Tashkent State University, Samarkand branch, G. S. Bitsadze, Yu. A. Budagov, V. B. Vinogradov, Yu. I. Davydov, V. P. Dzhelepov, A. B. Yordanov, V. M. Korolev (deceased), L. B. Litov, Yu. F. Lomakin, I. A. Minashvili, L. A. Permyakova, N. A. Rusakovich, A. A. Semenov, S. V. Sergeyev, S. Tokar, A. A. Feshchenko, V. B. Flyagin, Yu. N. Kharzheyev, and I. Ye. Chirikov-Zorin, Joint Institute of Nuclear Research in Dubna, A. A. Bogush, Yu. A. Kulchitskiy, A. S. Kurilin, L. G. Moroz, and M. N. Sergeyenko, Institute of Physics at BSSR Academy of Sciences in Minsk, V. Glinka, B. Sitar, and P. Strmen, Bratislava University imeni J. A. Komensky (Czechoslovakia), R. V. Tsenov, Sofia University imeni Kliment Okridsky (Bulgaria), J. Ferencey and J. Spalek, Institute of Experimental Physics at Slovak Academy of Sciences in Kosice (Czechoslovakia)—"Hyperon" Collaboration]

[Abstract] An experiment involving the $K^+ + A \rightarrow K^0 + X$ reaction (A = Be,Cu,Pb) at the 11.2 GeV energy level, within the range of K^+-meson fragmentation (Feynman variable $x_F \geq 0.4$ and transverse momentum $p_T \leq 0.5$ GeV/s^2), was performed in the "Hyperon" facility at the Serpukhov Institute of High-Energy Physics. The experiment was performed using a beam of positively charged particles with 11.2 GeV/s momentum, the particles not being segregated and approximately 6.5 percent of them being K^+-mesons. The magnetooptic channel (No 18) of the particle accelerator, located on the inside of the accelerator ring, contained three internal targets, a momentum collimator, two magnets guiding the incident particle beam and dispersing it on that collimator, a doublet of lenses focusing the incident particle beam onto that collimator, also two collimators orienting the axis of the incident particle beam and a doublet of lenses focusing it on a target. Before, a target was placed on a beam spectrometer for identification of incident particles and for measuring their momentum (maximum error 0.35 percent) as well as their coordinates and angles of incidence (maximum error about 0.3 mrad). This spectrometer had five Cerenkov counters (quartz optics and photomultipliers with a 56UVP window each, characteristic resolution 10^{-4} m^{-1}), four scintillation counters, four proportional chambers (two planes each, about 1400 recording channels altogether), and a superconducting magnet. Behind a target was placed a spectrometer of secondary particles coming from that target (momentum resolution 1 percent, error of exit angle measurement about 1 mrad). This spectrometer had a magnet, one proportional chamber (four planes), one summing proportional rod chamber, and one spark chamber before the magnet, three scintillation hodoscopes (32 elements 40 mm wide, 16 elements 150 m wide, 64 elements 60 mm wide), two spark chambers, two proportional rod chambers, and a wide-aperture (0.8x2.4 m^2) eight-channel Cerenkov-threshold gas counter behind the magnet. Upon injection of 1.3×10^9 K^+-mesons, there were recorded 2.1×10^6 events of the $K^+ + A \rightarrow$ two charged particles reaction on Be, Cu, and Pb targets. An evaluation of the data, including their statistical analysis, indicates that the doubly differential

cross-sections $d^2\sigma/dx_F dp_T^2$ mb.s^2/GeV for K$^+$A-interaction on these targets with x_F from 0.45 to 0.95 and p_T from 0.05 to 0.45 GeV/s depend on A according to the relation $d^2\sigma/dx_F dp_T^2 = CA^{\alpha}$ ($\alpha = f(x_F, p_T)$). The doubly differential invariant cross-sections $F(x_F, p_T)$ thus also depend on A, the relation $F(x_F,p_T) = F_0 A^{\alpha-\beta(1-x_F)^n}(1 - x_F^n \exp[-Bp_T^2]$ most closely fitting the data with $\alpha = 1.43+/-0.15$, $\beta = 0.084+/-0.006$, $n = 0.42+/-0.02$, and $B = 7.4+/-0.4$ (GeV/s^{-2}). The invariant cross-sections $F(x_F$ are independent of A, the relation $F(x_F) = C(1 - x_F)^n$ most closely fitting the data with $n = 0.42+/-0.03$ for the Be target and $n = 0.44+/-0.07$ for both Cu and Pb targets ($0.29+/-0.07$ for a H_2 target). The differential cross-sections $d\sigma/dp_T^2$ cross-sections depend on A, the relation $d\sigma/dp_T^2 = A \exp[-Bp_T^2]$ most closely fitting the data with $B = 8.2+/-1.1$ (GeV/s)$^{-2}$ for the Be target and $7.1+/-1.3$ (GeV/s)$^{-2}$ for both Cu and Pb targets ($7.6+/-0.9$ (GeV/s)$^{-2}$ for a H_2 p-target). Absorption by a target was corrected for in two ways: 1) on the basis of known cross-sections for absorption of K$^+$-mesons and $\pi^{+/-}$-mesons, 2) by extrapolation to "zero" target thickness. The acceptance $\varepsilon(x_F, p_T)$ was calculated by the Monte Carlo method, taking into account the width of the incident K$^+$-meson beam, dimensions and positions of the detectors, characteristics of the magnetic field, decay of $\pi^{+/-}$-mesons, triggering mode for sampling the events, and the data processing criteria. The authors thank Yu. D. Prokoshkin for support, S. P. Zhunin, N. P. Mashkov, and M. V. Tikhonov for installation of the detectors and assistance in operating them, and V. A. Uvarov for supplying data on production of K^0-mesons in K$^+$p-interactions with 16 GeV/s momentum. Figures 7; tables 5; references 21.

Quantum Solitons in Nonlinear σ-Model as Model of Baryons

927J0007C Moscow YADERNAYA FIZIKA in Russian Vol 53 No 2, Feb 91 pp 552-561

[Article by A. P. Kobushkin and N. M. Chepilko, Institute of Theoretical Physics at UkSSR Academy of Sciences, K. Fujii, University of Hokkaido, Sapporo (Japan)]

[Abstract] Following an earlier analysis of the quantum mechanism of soliton stabilization and its demonstration on radially vibrating solitons in the nonlinear SU(2) σ-model, this model is shown to be usable as a model of baryons. Nonperturbative quantization of radial vibrations of a chiral "hedgehog" field having already been shown to stabilize three-dimensional solitons, which nevertheless vanish at the h-bar $\to$ 0 limit, quantum vibration modes in the SU(2) σ-model are now considered and their effective Lagrangian $L_{vib}(\tau)$ as a function of time τ is obtained by reducing the problem of dynamics of such a chiral field in the Minkowski space-time $x^{\alpha} = (ct,x)$ ($\alpha = 0,1,2,3$ and $ct,x = c\tau,\lambda(\tau)z$) to its static "hedgehog" configuration. The equation of that chiral field is then obtained by equating the differential $\delta_{\theta}L_{vib}(\tau)$ to zero (θ - chiral angle). Addition of the standard mass term to the left-hand side of this equation changes the asymptotic behavior of the $\theta = \theta(z)$ function in the vibrating z-space. Subsequent quantization of the rotation of vibrating solitons in the nonlinear SU(2) σ-model reveals that quantum solitons always have a nonzero spin s and an isospin squared $T^2 = (h\text{-bar})^2 s(s + 1)$ ($s = 1/2,1,3/2,...$), thus also vanish at the h-bar $\to$ 0 limit. These solitons are stationary with topological charge p and inertial mass m_s, all their properties being expressible in terms of a single parameter which is the charged-pion decay constant f_{π}. They can therefore serve as a model of baryons more adequate than the Skyrme model. Figures 2; tables 1; references 9.

Interaction of Relativistic Particles and Strong Optical Interference Fields

927J0016A Moscow ZHURNAL EKSPERIMENTALNOY I TEORETICHESKOY FIZIKI in Russian Vol 99 No 6, Jun 91 pp 1668-1678

[Article by A. V. Andreyev and S. A. Akhmanov, Moscow State University imeni M. V. Lomonosov]

[Abstract] Interaction of relativistic charged particles and high-intensity light pulses is analyzed theoretically, specifically considering a beam of relativistic electrons in a strong electromagnetic interference field. The equations of electron ballistics in such a field are formulated in a three-dimensional Cartesian system of coordinates, assuming first that the interference field is a transverse electric one and that a relativistic electron enters in the direction in which this field moves. Extension of the analysis on this basis leads to a new mechanism of channeling such electrons and attendant emission of polarized radiation by them in the process in accordance with Doppler's law at harmonic and combination frequencies. The possibility of parametric resonance is predicted and the necessary field intensity is established, collimation of the electrons taking place under far-from resonance conditions as their transverse vibrations are attenuated by their radiation emission. Assuming next that the interference field is a transverse magnetic one, bunching of electrons in a relativistic beam by such a field is predicted and the threshold field intensity is established which separates the far-above resonance condition for bunching from the far-below-resonance condition for entrapment in the potential well. Axial channeling of relativistic electrons in a nondiffracting light beam is then predicted on the basis of vector wave equation for cylindrical waves, a complete solution to this equation being obtainable in analytical form upon representation of the wave field in the form of two components: a transverse electric wave and a transverse magnetic wave, each expressible as a solution to the scalar wave equation. In conclusion is considered interaction of relativistic electrons and surface electromagnetic waves, in which case parametric resonance can occur with a light beam of moderate intensity. This is demonstrated on an electron beam propagating along the surface of a medium which has become a waveguide for an electromagnetic wave incident at an angle insignificantly larger than the critical total-reflection angle.

Numerical estimates indicate that relativistic electrons are much more likely to become channeled in an optical interference field than in a crystal, inasmuch as no dechanneling whatsoever will occur in such a field. Figures 1; references 10.

On Effect of RF Electromagnetic Field on Tunneling Transitions Between Two Localized States

927J0033A Moscow YADERNAYA FIZIKA in Russian Vol 54 No 1(7), Jul 91 pp 69-79

[Article by F. O. Aleksandrov, G. L. Klimchitskaya, V. M. Mostepanenko, Leningrad Technological Institute]

[Abstract] Studies of the effect of external fields on various quantum processes and the new physical phenomena and results discovered by different authors in these studies are discussed. Quantum particle tunneling between two localized states in two potential wells with a zero radius under the effect of static and radio-frequency electric fields are investigated using the example of a simple one-dimensional problem. The results obtained herein also remain valid in the case of an arbitrary electric field. The effect of alternating external fields on the tunneling phenomenon was examined for the purpose of clarifying some problems of nuclear physics—nuclear α-decay stimulation and fusion reactions—and scanning tunnel microscopy of the surface of dielectrics. The tunneling current is computed for one-dimensional potential wells of zero radius whereby wells of equal and varying intensity are examined. Given a proper alternating field frequency, resonance develops in the latter case. The resulting current values make it possible to draw the conclusion that the tunneling current amplification by the alternating field may be observed experimentally. The studies demonstrate that in the resonance case, a high tunneling current (on the order of several nanoamperes) appears at an unusually long distance between the wells, i.e., close to 15 angstrom. The authors are grateful to V. N. Ostrovskiy and V. I. Popov for useful discussions. References 15: 13 Russian, 2 Western.

Complete Disintegration of Nuclei

927J0033B Moscow YADERNAYA FIZIKA in Russian Vol 54 No 1(7), Jul 91 pp 125-127

[Article by I. Bobodzhanov, Engineering Physics Institute at the Tadzhik Academy of Sciences]

[Abstract] Complete disintegration of nuclei—a phenomenon where target nuclei break up, mostly into individual particles, under the effect of various colliding projectiles, such as particles and nuclei (*p, d, t*, He, and Li)—is discussed and the results of an investigation of complete heavy emulsion nuclei (Ag, Br) disintegration under the effect of various colliding nuclei conducted in 1973-1989 at the Joint Institute for Nuclear Research and the Engineering Physics Institute at the Tadzhik Academy of Sciences as well as other organizations are cited. The studies revealed an empirical relation between the probability of complete heavy emulsion nuclei disintegration and the atomic weight of the projectile nucleus (all the way from a proton to a silicon nucleus) within the 4.1-4.5 GeV/c per nucleon primary momenta range. Stacks of a standard BR-2 100x100x0.6 mm^3 photo emulsion as well as BR-2Pb lead-containing photo emulsion were irradiated in accelerators in the experiments. Figures 1; tables 5; references 9.

Interaction of Massive Neutrinos With Planar Wave Field Allowing for Abnormal Magnetic Moment

927J0033C Moscow YADERNAYA FIZIKA in Russian Vol 54 No 1(7), Jul 91 pp 162-166

[Article by V. V. Skobelev, Moscow State Correspondence Teachers Institute]

[Abstract] The interest in the effects of neutrino interaction with a planar wave external field is attributed to the possibility of clarifying the characteristics of various types of particles, e.g., the mass and magnetic and electric moments and such astrophysical applications as the latent mass and sterilization effects under the stimulating effect of external field. The probabilities of the $\nu_i \rightarrow \nu_i\nu_j\nu_j$ and $\nu\nu \rightarrow \gamma$ transitions with massive neutrino in the field of a linearly polarized planar wave and static crossed field are analyzed using known methods. The corresponding contributions at $m_i >> m_j$ and $m_i << m_j$ and threshold values are compared in the existing experimental environment and from the astrophysical viewpoint. It is shown that at the existing and especially anticipated detection levels, four-neutrino crossing processes cannot affect the balance of different types of neutrino, even in the astrophysical interpretation, due to these processes' equal probability. References 8: 6 Russian, 2 Western.

New Nonperturbative Approach to QCD and Its Applications in Hadron Physics

927J0033D Moscow YADERNAYA FIZIKA in Russian Vol 54 No 1(7), Jul 91 pp 192-223

[Article by Yu. A. Simonov, Theoretical and Experimental Physics Institute, Moscow]

[Abstract] A new nonperturbative approach to quantum chromodynamics (KKhD) recently developed in a series of original studies hereinafter referred to as the vacuum correlators method (MVK) is systematically reviewed. The method makes it possible to consider both small and long ranges and compute any physical amplitude in QCD through perturbative corrections and nonperturbative dynamic contributions which are defined by the so-called irreducible gluon field correlators, i.e., vacuum means. It is demonstrated that lower correlators make the principal contribution and, consequently, the VCM can be reduced to a rather simple workable computation

procedure where all observations may, in principle, be expressed through one or two correlators. The method is applied to heavy quarkonia, mesons, baryons, and glueballs thus creating a consistent pattern of nonperturbative physics which confirms the experiment. The method's procedure is based on three fundamental formalisms: the so-called Fock-Dirac (Feynman-Schwinger) (FD) representation of the Green function; the cluster (cumulant) expansion of Wilson's loop making it possible to express the Green function through vacuum correlators; and the relativistic proper time formalism for several light quarks or gluons interacting with each other and with vacuum fields. The author is grateful to L. MacLerran and H. G. Dosch. Figures 8; tables 4; references 64: 10 Russian, 54 Western.

Diffraction Interaction of ^{6}Li Ions With Atomic Nuclei and Polarization Phenomena

927J0035A Moscow YADERNAYA FIZIKA in Russian Vol 53 No 6, Jun 91 pp 1559-1566

[Article by M. V. Yevlanov, A. M. Sokolov, V. K. Tartakovskiy, Nuclear Research Institute at the Ukrainian Academy of Sciences and Kiev State University]

[Abstract] Polarization phenomena which accompany the elastic scattering and dissociation of ^{6}Li ions by ^{12}C nuclei in a diffraction approximation of a perfect radiator with a sharp absorption edge is discussed and the differential cross section, polarization, and quadrupolarization of ^{6}Li ions during their diffraction elastic scattering on ^{12}C nuclei and the differential cross section of the diffraction dissociation of ^{6}Li ions in the field of ^{12}C nuclei into a deuteron and an α-particle as well as polarization and quadrupolarization of the resulting deuterons at a 150 MeV incident particles energy are calculated in a diffraction model with a diffuseness nucleus target boundary. Vector and tensor polarizations of lithium ions are calculated and compared to experimental data. The analytical results are found to be adequately consistent with the results of very complex calculations performed by Y. Sakuragi *et al.* using the coupled channels method. Figures 6; references 5: 4 Russian, 1 Western.

Comments on Models With Light ZKM Neutrino With High Magnetic Moment

927J0035B Moscow YADERNAYA FIZIKA in Russian Vol 53 No 6, Jun 91 pp 1632-1637

[Article by M. I. Vysotskiy, M. A. Stefanov, Theoretical and Experimental Physics Institute, Moscow and Physics Institute at the USSR Academy of Sciences]

[Abstract] Ways of explaining the anticorrelation of the solar neutrino flux observed by Davis *et al.* with the magnitude of solar activity by assuming that neutrinos possess a diagonal or transient magnetic moment on the order of $(10^{-12} - 10^{-10})\mu_B$ where μ_B is Bohr's magnetron are suggested. The recently proposed models of Zeldovich-Konopinskiy-Makhmud (ZKM) neutrinos characterized by $\mu_\nu \approx 10^{-11}\mu_B$ and $m \leq 10$ eV are discussed and compared to the Ecker, Grimus, and Neufeld model, the Leurer and Markus model, and the supersymmetric Babu and Mohapatra model. It is shown that the latter is not self-consistent. Symmetry is discovered in the Ecker, Grimus, and Neufeld model which, in reality, ensures that m is small. The possibility of attaining a wider range of neutrino mass and new scalar particles in the Leurer and Markus model is indicated. The most significant feature of the above models is the integrity of the ZKM's $U(1)$-symmetry which prohibits the bifurcation of masses of the two neutrino states. The most important feature of models with a horizontal symmetry is the mechanism of μ and e mass bifurcation related to the neutrino mass magnitude. Thus it is shown that the problem of natural generation of different μ and e masses still remains unresolved. Figures 3; references 11: 2 Russian, 9 Western.

Spontaneous Diffraction in Anisotropic Nonlinear Media in Symmetry-Wise "Forbidden" Configurations

917J0126B Kiev UKRAINSKIY FIZICHESKIY ZHURNAL in Russian Vol 36 No 4, Apr 91 pp 501-504

[Article by M. Yu. Gulkov and S. G. Odulov, Institute of Physics, UkSSR Academy of Sciences, Kiev]

UDC 535.36:535.21:778

[Abstract] Self-diffraction of extraordinary waves was observed in $LiNbO_3$:Fe crystals, photorefractive crystal of the 3m class, in a configuration "forbidden" as regards holographic recording. Two beams of 440 nm light from a He-Cd laser approximately 1 mm in diameter were without widening applied to a $LiNbO_3$:(0.03 wt.%) Fe crystal, a 2 mm thick plate with 10 mm square faces, at various angles θ of incidence in a plane perpendicular to the C-axis. After some time, tens of seconds, light-induced structures were found to form which coupled waves of the two recording beams by a diffraction mechanism: while one of them was covered, waves with the same polarization propagated in the same direction after having been diffracted by the other beam. This was observed in X-cut and Y-cut crystals. The diffraction efficiency was low, approximately 0.1 subject to systematic errors. Not only diffraction was taking place, moreover, but also light-induced scattering. Diffractional coupling of waves incident on such crystals in a "forbidden" configuration can, therefore, be regarded as a parametric process in which scattered waves participate. A theoretical model is constructed on this basis, assuming a conical scattering pattern where a wave coherent with waves in both recording beams forms an interference pattern with each. This model is consistent with a two-stage transient recording process in which the diffraction efficiency increases much faster according to the approximate relation $\eta \approx a_4 t^4$ than according to the approximate relation $\eta \approx a_2 t^2$ characterizing a conventional simple transient recording process. The rate of increase of diffraction efficiency depends nonmonotonically on angle α between the C-axis of the crystal and the planes of equal phase difference in the grating formed by the recording beams. Calculations covering the $\alpha = -50°$-$(+50°)$ range indicate that both coefficient a_4 and the correlation coefficient r_4 which characterizes the degree of accuracy of the $\eta \approx a_4 t^4$ approximation increase as the "forbidden" configuration corresponding to $\alpha = 0$ is approached, while the coefficient a_2 does not change appreciably and the correlation coefficient r_2 dips to a low minimum when $\alpha = 0$. The diffraction efficiency η, accordingly, increases as t^4 when $\alpha = 0$ and as t^2 when $\alpha > 20°$ or $\alpha < -20°$. Any wave coherent with the incident ones and lying in the plane of their incidence can, therefore, couple them even when the configuration is a "forbidden" one. The diffraction efficiency η depends also on the angle of incidence θ, this dependence being monotonic with the efficiency decreasing as that angle is increased and the projection of the electric field vector of scattered waves onto the C-axis correspondingly decreases. As the angle of incidence is increased, moreover, the photogalvanic current decreases. Increasing the angle of incidence thus influences the recording process by limiting the field of the space charge and influences the readout process by decreasing the modulation of the refractive index Δn by the electrooptic effect. Theoretically η should be proportional to $\cos^4(\theta/2)$ in a two-stage process. In an experiment the dependence of η on θ was stronger, evidently due to these attendant effects of increasing the angle θ. The authors thank Yu. N. Parkhomenko for helpful discussion. Figures 3; references 5.

Saturation of Coherent Amplification of Ultrashort Pulses in Inverted Medium

917J0127B Moscow PISMA V ZHURNAL EKSPERIMENTALNOY I TEORETICHESKOY FIZIKI in Russian Vol 53 No 8, 25 Apr 91 pp 400-402

[Article by S. V. Sazonov, Institute of Pacific Oceanography, Far Eastern Department, USSR Academy of Sciences, Vladivostok]

[Abstract] Propagation of an ultrashort laser pulse through a population-inverted two-level solid-state medium is analyzed on the basis of the applicable system of four Maxwell-Bloch equations for the time derivatives of quantum-mean Pauli operators. In this system of equations there appear two constants, the effective dipole-dipole interaction constant J and a phenomenological constant γ which represents losses due to absorption and scattering at extraneous atomic transitions in the medium. The system of equations is solved by integration for the electric field and the inversion, assuming that $\Omega \geq \omega_0 \geq J$ (ω_0 - frequency of atomic transition, d - dipole moment of atomic transition, $\Omega = dE/h$, E - electric field component in direction of the dipole moment, h - Planck constant). Numerical estimates indicate that amplification of a pulse can become saturated within a distance $z = 10$ cm, which corresponds to a propagation time of approximately 300 ps and thus much shorter than the characteristic time of spontaneous emission. It therefore should be possible to detect saturation of amplification of ultrashort pulses experimentally, also to evaluate J and γ by measuring both the width and the amplitude of a dissipative soliton as it exits from the medium. References 10.

Experimental Bistable Inversion State Detection in Traveling Wave Maser (Letter to Editor)

917J0130A Kiev UKRAINSKIY FIZICHESKIY ZHURNAL in Russian Vol 36 No 6, Jun 91 pp 826-828

[Article by D. N. Makovetskiy, A. A. Lavrinovich, Radiophysics and Electronics Institute at the Ukrainian Academy of Sciences, Kharkov]

UDC 537.635:621.375.8

[Abstract] The formation of two independent branches of nonequilibrium, or inversion, states of paramagnetic

centers as a result of the paramagnetic's saturation or pumping under the self-effect of a coherent pumping wave through the electron spin-system is discussed. The first experimental observation of a pair of independent stable steady-state inversion branches in masers' active medium whereby transitions between the branches are manifestly hysteretic is reported. The experiments were performed in a real paramagnetic traveling wave millimeter band maser (MBV) in which additional conditions for efficient pumping field self-action through the system of H-spins processing in the static magnetic field were created. Transitions between the branches were accompanied by critical retardation processes. The maser's active medium was a crystal of Fe^{3+}:Al_2SiO_5 andalusite which was pumped by a diffraction radiation generator at a 143.6 GHz frequency. It is shown that each branch maintains the linear traveling wave signal gain mode. References 12: 11 Russian, 1 Western; figures 1.

New Approaches to High-Efficiency High-Resolution Resonance Ionization Spectroscopy

917J0131A Leningrad PISMA V ZHURNAL TEKHNICHESKOY FIZIKI in Russian Vol 17 No 11, Jun 91 pp 5-8

[Article by G. D. Alkhazov]

[Abstract] The method of resonance ionization spectroscopy first used at the Leningrad Nuclear Physics Institute (LIYaF) to examine the properties of unstable nuclei and its application in laser spectroscopy are discussed. The possibility of further increasing both the method's efficiency and resolution is addressed. In so doing, two versions are considered: one is a modification of the traditional approach described by Zherikhin *et al* in *ZhETF* Vol 86, 1984, p 1249, in which an atomic beam formed in a vacuum by a hot metal tube from which it emerges is intersected at a right angle by several (three, as a rule) converging laser beams as a result of which the atoms are ionized, and the other is based on using the selective laser ion source proposed by the author earlier in which a laser radiation beam from three wide-band lasers tuned to three resonance frequencies is directly injected into a hot tube in which the nuclei under study are ionized. A case where the nucleus under study has a zero spin is analyzed. The results demonstrate that the first method makes it possible to substantially increase resolution and ensure a 10-100x increase in efficiency over traditional methods depending on the resolution requirement while the second method makes it possible to attain sufficient resolution which can be increased further but only at the expense of efficiency. References 2: 1 Russian, 1 Western; figures 1.

Fractal Fracture Dynamics

917J0131B Leningrad PISMA V ZHURNAL TEKHNICHESKOY FIZIKI in Russian Vol 17 No 11, Jun 91 pp 9-13

[Article by A. S. Balankin]

[Abstract] The fractal dimension of self-similar crack configurations and its relationship to the type of boundary value conditions which simulate various types of loading, i.e., tension, compression, shear, etc., and to the exponent of stress affecting the bond in the planar lattice is considered. The calculations made in *Fraktaly v fizike*, Moscow: Mir, 1988, pp 244-248 are repeated for a trigonal lattice with 100x100 dimensions in order to derive the dependence of fractal dimension on Poisson's ratio. It is shown that the geometric image of self-similar crack configurations is substantially determined by the symmetry imposed by the boundary value conditions due to the fundamental property of elastically isotropic media. Elastic properties of fractals and the results of numerical experiments and numerical simulation of percolation lattices as well as the general theory of isotropic fractal elasticity are reviewed on the basis of numerous sources. The behavior of percolation lattices is examined. Elastic deformation in the case of brittle failure is investigated and the fractal dimension of cracks is examined theoretically and experimentally; a comparison demonstrates an almost ideal consistency of the theory and numerical simulation results. References 17: 10 Russian, 7 Western; figures 1.

Compression of Sum-Frequency Pulses by Mixing Phase-Conjugate Waves in Nonlinear Crystals

927J0008A Vilnius LITOVSKIY FIZICHESKIY SBORNIK in Russian Vol 31 No 2, Mar-Apr 91 pp 199-205

[Article by G. Valiulis and A. Stabinis, Vilnius University]

UDC 621.373

[Abstract] Mixing of two phase-conjugate waves (frequencies ω_1,ω_2 in a crystal with quadratic nonlinearity and attendant generation of a sum-frequency (ω_3) wave are considered, subsequent three-wave parametric interaction providing a simple mechanism for compression of sum-frequency light pulses. Analysis of the process is based on the first-order dispersion theory, in the approximation of a given field of mixing waves. When the complex amplitudes A_{10} and $A_{20} = A_{10}^*$ of the mixing waves are even functions of time, then the sum-frequency wave with complex amplitude A_3 is shown to be the correlation function of the two mixing waves. In this case, provided that the correlation time of the sum-frequency signal pulse is much shorter than its duration and with a ratio of group velocities $m = v_{23}/v_{13} \approx -1$, it is possible to compress a phase-modulated light pulse into much shorter demodulated one. This is demonstrated on a Gaussian pulse with linear frequency modulation and an amplitude of the mixing waves $A_{10,20} = a_{10}\exp[-t^2(1 - i\gamma_{10})/\tau_{10}^2]$, such a pulse also being convertible in this way into one without phase modulation when $m \approx -1$ (widest spectrum) and when $m = 1$ (narrowest spectrum). The pulse demodulation factor γ_3/γ_{10} (function of m) and the pulse compression ratio

τ_3/τ_{10} (function of m and γ_{10}) are calculated for m from -2 to 2 (γ_{10} = 10), the compression ratio being maximum and the phase modulation vanishing when m = -1 and the compression ratio becoming zero when m = 1. The duration of a sum-frequency pulse and thus also the compression ratio are shown to be a function of the distance traveled by the pulse in the nonlinear medium. A computer-aided search for nonlinear media with dispersion characteristics necessary for this mode of pulse compression has revealed that the necessary conditions are realizable only for oe-e or eo-e interaction. The dependence of m on the degeneracy parameter $\kappa = \omega_1/\omega_3$ has been evaluated numerically for a KDP crystal and a sum-frequency wave of λ_3 = 0.53 μm light. With mixing waves of λ_1 = 0.97 μm radiation and λ_2 = 1.17 μm radiation, m = -1 is obtained here when κ = 0.454 in oe-e interaction. Figures 4; references 3.

Luminescence Spectrum of Heavily Doped InP

927J0008B Vilnius LITOVSKIY FIZICHESKIY SBORNIK in Russian Vol 31 No 2, Mar-Apr 91 pp 206-211

[Article by F. Alex and B. Lux, Center for Scientific Instruments at GDR Academy of Sciences in Berlin, A. Dargys, J. Kundrotas, and A. Cesna, Institute of Semiconductor Physics at LiSSR Academy of Sciences]

UDC 621.315.592

[Abstract] The luminescence of heavily doped n-InP:(S,Te) structures was studied in an experiment involving epitaxial n-InP layers with an electron concentration n = 1.9 x 10^{17} cm^{-3} and n-InP single crystals with electron concentrations n = 1 x 10^{18} cm^{-3} or n = 4 x 10^{18} cm^{-3}), an Ar-laser serving as the excitation source. The exciting radiation was transmitted to a specimen through a standard optical fiber with a 50 μm diameter core, the power density of this incident radiation being varied over the 0.1-1 W/cm^2 range and thus remaining suufficiently low for the form of the luminescence spectrum not to depend on it. Radiation generated in a luminescing specimen was extracted through a special optical fiber with a 440 μ diameter core to a spectrum analyzer with an MDR-23 monochromator and an FEU-112 photomultipler operating as photon counter. The luminescence spectra were recorded with the crystal lattice of each specimen at three temperatures: 300 K, 77 K, 4.2 K. The luminescence spectra of the two n-InP single crystals at 77 K and at 4.2 K contain emission bands with peaks within the 1.35-1.45 eV range associated with radiative transitions of electrons, either B-B transition from the conduction band to the valence band and subsequent recombination with holes in the valence band or A-transition from the conduction band to the acceptor (S or Te) level and subsequent recombination with holes on the acceptors. The luminescence spectrum of the epitaxial n-InP layer with its lattice at 4.2 K also includes an emission band associated with A-LO transition of electrons from the conduction band to the acceptor (S or Te) level and attendant emission of an optical photon. The spectra are compared with and found to agree quite closely with the theoretical spectra calculated according to the applicable relation for the intensity of luminescence due to recombination in semiconductors (G. Lasher and F. Stern; PHYSICS REVIEW Vol 133 No 2A, 1964) and with the results of earlier measurements (R. Schwabe, E. Haufe, V. Gottschalch, and K. Unger; SOLID STATE COMMUNICATIONS Vol 58 No 7, 1986). Considering that the conduction band and the impurity band merge as the donor concentration decreases as a result of compensation (D. A. Anderson and N. Apsley; SEMICONDUCTOR SCIENCE AND TECHNOLOGY Vol 1 No 3, 1986), the applicable dispersion law for these two merging band (A. Haufe, R. Schwabe, H. Fieseler, and M. Ilegems; JOURNAL OF PHYSICS: SOLID STATE PHYSICS Vol 21 No 15, 1988) and the density of states in them have been taken into account in the theoretical analysis. Figures 3; references 9.

Surface Acoustoelectric Interaction in Sb_2S_3 Single Crystals

927J0008C Vilnius LITOVSKIY FIZICHESKIY SBORNIK in Russian Vol 31 No 2, Mar-Apr 91 pp 220-228

[Article by A. Jucys, Vilnius University]

UDC 534.23:541.183

[Abstract] An experimental study of ferroelectric semiconductor crystals with a strongly anisotropic and temperature-dependent dielectric permittivity was made concerning surface acoustoelectric interaction in such crystals with and without photoexcitation. Slices of Sb_2S_3, 2.7 mm thick with a 5x6 mm^2 large (001) mirror surface and the C-axis parallel to the 6 mm long edges, had been cut from an Sb_2S_3 single crystal. Such a slice was suspended centrally and exactly parallel above a much longer than 6 mm YZ-cut $LiNbO_3$ crystal plate serving as sound guide. On the upper surface of this plate facing the Sb_2S_2 crystal slice were mounted three transducers. At one end, beyond the crystal slice, were mounted an interdigital 20 MHz radiator-transducer generating surface acoustic waves in pulses of 1.7 μs duration at a repetition rate of 50 Hz and an interdigital 18.6 MHz radiator-transducer generating surface acoustic waves in the continuous mode. The generated sound beams were 79.5 mm wide. At the other end, also beyond the crystal slice, was mounted a 20 MHz receiver-transducer. Electric signals were picked up by a pair of metal electrodes, a grounded one above the Sb_2S_3 crystal slice separated from it by a narrow vacuum gap and a translucent one centrally underneath the $LiNbO_3$ plate making direct contact with its lower surface. Pulses of transverse acousto-e m.f. were recorded through an emitter-follower transistor amplifier in the form of acoustoelectric voltage pulses. Positive video pulses generated in an Sb_2S_3 crystal slice were picked up by the

translucent lower electrode. Attenuation of surface acoustic waves upon their passage across an Sb_2S_3 crystal slice was recorded by the receiver-transducer. Absence of contact tabs on that crystal slice and resulting absence of constant electrostatic fields in it ensured a distortionless free surface. Measurements were first made at 289 K temperature, for determining the dependence of the transverse acousto-e.m.f. and of the absorption of sound waves by holes on the intensity I of photoexcitation by white light under a vacuum of 7 μPa. The dependence of the amplitude of transverse acoustoelectric voltage pulses $V_{AE,t}$ on the light intensity was found to follow a hysteresis loop, with $V_{AE,t}$ peaking to a 0.552 mV maximum at I ≈ 80 W/cm² when I was increased from zero up and only to about 0.4 mV maximum when I was decreased back to zero. The dependence of $V_{AE,t}$ on the length of holding time in darkness after a 30 min long exposure to light of I = 220 W/cm² intensity was then determined on the basis of measurements made after black-out, $V_{AE,t}$ having been found to reach its 0.3 mV saturation level much sooner after a 0.5 s long black-out than after a 17 min long one. The photosensitivity of the Sb_2S_3 crystal surface $\gamma = 20$ ($\log V_{AE,t}^{light}/\log V_{AE,t}^{dark}$) was measured at temperatures covering the 289-430 K range and found to decrease from 2 db at 289 K to zero at 321 K and then become negative with an approximately -2.5 dB maximum at about 360 K. The temperature dependence of $V_{AE,t}$ measured without photoexcitation was found to include a hysteresis loop with a crossover at 321 K, $V_{AE,t}$ peaking to a 0.94 mV maximum at 408 K as the crystal surface was heated to 430 K and then passing through two lower peaks before passing through the 321 K crossover point (same amplitude as during heating) as the crystal surface was cooled back to 289 K. When measured with photoexcitation of 230 W/cm² intensity, $V_{AE,t}$ passed through two peaks at 338 K and at 385 K during heating and then decreased monotonically during cooling. The amplitude of $V_{AE,t}$ at 321 K was the same with and without photoexcitation. These trends can be explained by the fact that the transverse acousto-e.m.f. is inversely proportional to the surface dielectric permittivity of an Sb_2S_3 crystal and that, as the surface of such a crystal is heated up to 321 K, its electrical conductivity increases while its photosensitivity decreases to zero. As to the temperature dependence of the coefficient α of sound absorption by holes with and without photoexcitation, it was found to include hysteresis loops similar but not identical to those characterizing the temperature dependence of $V_{AE,t}$. Further measurements pertained to the "internal" acoustoelectric field induced in the acoustoelectric interaction layer by surface acoustic waves and the dependence of its intensity (resultant of transverse and parallel components) on the intensity of the surface acoustic waves. That field intensity was found to peak sharply to over 0.2 V at a 4.5 W/m wave intensity and then to drop as sharply to about 0.05 V at a 10.7 W/m wave intensity, before rising again but monotonically to a saturation level of about 0.5 V as the intensity of surface acoustic waves was further raised to 155 W/m. As the acoustoelectric field intensity increased from zero to 0.5 V, the amplitude of transverse acoustoelectric voltage pulse first increased to a 0.102 mV maximum at the 0.284 V field intensity and then decreased to zero at the 0.5 V field intensity. The amplitude of the transverse acoustoelectric voltage pulse was, furthermore, found to increase with longer time of action of surface acoustic waves in the continuous mode: up to 0.873 mV after a 900 s long action of surface acoustic waves of 180 W/m intensity. The author thanks J. Grigas for interest and helpful discussion. Figures 8; references 13.

Quantum Fluctuations Annihilate Optical Soliton

927J0009E Leningrad PISMA V ZHURNAL TEKHNICHESKOY FIZIKI in Russian Vol 17 No 7, 12 Apr 91 pp 61-65

[Article by A. V. Belinskiy]

[Abstract] Already having been established that quantum effects attending propagation of a Schroedinger soliton through an intrinsic optical fiber eventually annihilate such a soliton, this phenomenon is further analyzed for an explanation of its nature. The evolution of such a soliton in the optical field of an infinitely long lossless fiber is described by the nonlinear Schroedinger equation, both the photon annihilation operator $\Phi(t,x)$ and the photon generation operator $\Phi^*(t,x)$ appearing here in the Heisenberg representation as functions of normalized time t representing the distance traveled and of the coordinate x representing the distance from the pulse crest. An expression describing the form of the pulse envelope is derived, an approximate one with respect to the average number of photons $n_0 >> 1$ only and without any other constraints. An analysis of this expression indicates a continuous further blurring of such a soliton as t increases, the characteristic doubling-in-breadth time t_d depending on the value of the nonlinearity parameter c in that Schroedinger equation and on the width Δp of the moment distribution ($t_d \approx 2n_0 c[]gDp$ when $\Delta p >> c[.]$ $t_d \approx 2^{1/2}/n_0 c[]gDp$ when $\Delta p \approx c[.]$ $t_d \approx 3^{1/2}/n_0 c[]gDp^2$ when $\Delta p << c$. The fact that the "self-cleansing" mechanism does not operate here is explained on the basis of a multimode model of a soliton with a classical regular cosh-envelope modulated by noise in the form quantum vacuum fluctuations, "riddance" of fluctuations following but never fully compensating their "buildup". This is demonstrated mathematically by linearization of that Schroedinger equation with respect to fluctuation components of the soliton and, for simplicity considering single-mode interaction. The noise intensity is shown to continuously rise, not only because parametric four-photon interaction results in an irreversible transfer of photon from the regular component to the fluctuation component but also because the soliton acts as a pump which irreversibly amplifies the vacuum noise while becoming depleted in the process so that the total number of photons remains constant (in a lossless system). Figures 1; references 7.

Experimental Determination of Optical Properties Quartz-Fiber Thermal Insulation

927J0011C Moscow TEPLOFIZIKA VYSOKIKH TEMPERATUR in Russian Vol 29 No 1, Jan-Feb 91 pp 134-138

[Article by A. V. Kondratenko, S. S. Moiseyev, V. A. Petrov, and S. V. Stepanov, Institute of High Temperatures, USSR Academy of Sciences]

UDC 536.2.022

[Abstract] An experimental study of quartz-fiber thermal insulation was made for a determination of its optical properties, specifically its effective absorption coefficient k (cm^{-1}) and its radiation diffusion coefficient D (cm), the method being based on application of Fick's law to radiation diffusion in optically dense strongly scattering but weakly absorbing materials such as quartz fiber and solving the equations of diffusion for a cylinder of finite length with a flat base at each end. Solution of these equations yields an expression for the bihemispherical transmittance as the ratio of energy leaving to energy isotropically entering such a cylindrical fiber. Considering that thermal insulation made of this material consists of random oriented fibers which fuse together at the contact sites and thus form a rigid three-dimensional structure, one produces it by cutting quartz fibers to an about 100:1 length-to-diameter ratio and then mixing them with a binder. The cake is then fired and sintered, the fibers becoming thicker in the process as a result of mass active mass transfer and some of the thinner ones turning into beads. Addition of a boron compound during firing increases the mechanical strength of the insulation, owing to formation of boron oxide B_2O_3 and its reaction with SiO_2 so that a borosilicate glass is produced. Although this glass can be highly nonhomogeneous with a high B_2O_3 content in some places on the surface to pure SiO_2 in most places, depending on various random factors, its refractive index varies within a very narrow range only: from 1.459 (SiO_2) to 1.463 (B_2O_3) for 0.63 μm light. The experiment was performed in a test stand consisting of a master sphere and an integrating one, lasers as sources of collimated radiation, an interference filter, a light modulator, an interference filter, a beam-splitter plate, a focusing lens, and a set of radiation detectors. Measurements were made at room temperature (295 K) in 0.63 μm visible light, also in 1.15 μm and 3.39 μm infrared light. Cylindrical specimens 30 mm in diameter with 4-50 mm wall thickness consisted of fibers of 10 size fractions covering the 0-5.0 μm range, 42 percent of them in the 1.5-2.0 μm and 3.0-3.5 μm diameter fractions. One and the same specimen was used for plotting the polar diagram of its directive hemispherical transmittance for each of the three wavelengths. On the basis of the data have been calculated the effective absorption coefficient k and the radiation diffusion coefficient D, also the attenuation coefficient $\zeta = (k/D)^{1/2}$, for each of the three wavelengths. A formula is proposed for the temperature dependence of the effective absorption coefficient by using the absorption coefficient of pure quartz glass (S.V. Stepanov: TEPLOFIZIKA VYSOKIKH TEMPERATUR Vol 26 No 1, 1988) and assuming that the absorption coefficient of impurities is only weakly temperature dependent. The temperature dependence of the radiation diffusion coefficient may be ignored, inasmuch as this coefficient is determined essentially by the structural characteristics of the material such as the size of fibers and by its refractive index only. Figures 1; tables 2; references 12.

Measuring Displacement of Objects by Speckle Photography With Use of Fiber Optics

927J0013A Leningrad PISMA V ZHURNAL TEKHNICHESKOY FIZIKI in Russian Vol 17 No 2, 26 Jan 91 pp 15-19

[Article by Yu. A. Bykovskiy, Yu. N. Kulchin, A. I. Larkin, M. V. Marchenko, V. L. Smirnov, and V. N. Sorokovikov]

[Abstract] Use of multimode optical fibers for measuring displacement of objects by speckle photography is considered on account of their ability to transmit coherent light over long distances without noticeable attenuation. The light emerging from the fiber exit, where it forms a speckle pattern, can then be collimated by means of cylindrical gradient lenses. As an object moves vertically through some distance while the phase of each wave participating in formation of the speckle pattern remains unchanged, the speckle pattern moves through an equal distance measurable on a photographic film exposed once with the object in its initial position and then again with the object in its final position. On the subsequently developed film there appear two identical speckle patterns separated from one another, their Fourier spectrum consisting of a bright spot in the center on a speckle background modulated by Young's interference fringes with a period Λ proportional to the displacement Δ of the object. That displacement can thus be obtained from the relation $\Delta = F\lambda/\Lambda$ (λ - wavelength of light, F - focal length of Fourier objective) and the fringe contrast will be $c = (I_{max} - I_{min})/(I_{max} + I_{min})$ ($I_{max,min}$ - first intensity maximum and minimum in interference pattern). The contrast thus also depends on the displacement of the object, as a periodic function of the latter. The validity of these relations has been confirmed by an experiment involving use of an He-Ne laser as source of 0.63 μm light, a microobjective lens, and a bundle of 1.5 m long multimode fibers with 200 μm in diameter quartz cores acting as a multiple-beam interferometer. In order to avoid possible decorrelation of the speckle pattern, owing to the high sensitivity of multimode fibers to vibration and other mechanical effects, the bundle of such fibers was subsequently replaced with a composite optical channel consisting of a 2.5 m long lead-in single-mode fiber spliced to a 1.5 cm long lead-out gradient-index multimode fiber with a 140 μm in diameter. Both fibers and a 1.6 mm in diameter cylindrical gradient lens

behind the exit were all matched in glass capillaries and mounted so as to form a monolithic assembly. Figures 2; references 8.

Adaptive Holographic Interferometer for Measurement of Submicron Step Displacements

927J0013D Leningrad PISMA V ZHURNAL TEKHNICHESKOY FIZIKI in Russian Vol 17 No 2, 26 Jan 91 pp 32-35

[Article by Yu. O. Barmenkov and N. M. Kozhevnikov, Leningrad State Engineering University]

[Abstract] An adaptive holographic optical interferometer for measurement of submicron step displacements in nonlinear media containing bacteriorhodopsin is described, high-precision phase modulation of the reference beam providing the necessary immunity of such measurements to low-frequency noise. Adaptive stabilization of its operating point in space and time is effected by means of dynamic holograms. This interferometer, mounted on a heavy base with vibration isolators, operates with a 1.6 mW LGN-207B He-Ne laser as source of 0.63 μm light. A semitransparent plate splits the laser beam into two. Both the reflected one and the transmitted one are then redirected, each by another opaque plane mirror behind that plate, so that they will converge on the layer of a photorefractive medium and then diverge upon leaving that medium for a differential photodetector. The mirror which redirects the reflected light beam leans against a piezoelectric transducer which receives a sinusoidal 20 Hz voltage from a harmonic oscillator. The mirror which redirects the transmitted light beam leans against a piezoelectric transducer which receives square voltage pulses with amplitude regulation from a square-wave generator. These voltage pulses, converted into pressure pulses, cause normal displacements of that mirror which are to be measured. The photodetector is designed to suppress the in-phase signal by at least 40 dB. With a film of a photorefractive polymer containing bacteriorhodopsin as slightly nonlinear recording medium, the second-harmonic signal is amplified and then recorded by a synchronous detector while also being displayed on the screen of oscillograph for amplitude measurement. The interferometer has a sensitivity threshold for submicron displacements in even such a slightly nonlinear medium. Photorefractive sillenite crystals with an appreciable nonlocal nonlinearity and an adequate response speed even in the absence of an electric field may be better recording media. With such a medium, the signal can be recorded at the fundamental frequency of reference-beam phase modulation. Figures 2; references 7.

Tomographic Temperature Field Reconstruction in Gaseous Medium From Data of Double-Angle Spectroscopy Measurements

927J0030B Moscow TEPLOFIZIKA VYSOKIKH TEMPERATUR in Russian Vol 29 No 2, Mar-Apr 91 pp 345-349

[Article by M. N. Rolin, N. L. Yadrevskaya, Heat and Mass Transfer Institute at the Belorussian Academy of Sciences]

UDC 533.9

[Abstract] The methods of diagnosing gas and plasma flows on order to reconstruct the spatial distributions of physical parameters with the help of computer-aided tomography (CAT) is discussed and a method of reconstructing the temperature pattern in gaseous or plasma media on the basis of emission or absorption spectroscopy at two angles which makes it possible to compensate for the shortage of data on the object under study due to the small number of angles with data obtained for a number of wavelengths is proposed. The method requires that the optical properties of the media be a function of a sole parameter, i.e., temperature. If this condition is met, local thermodynamic equilibrium exists in the media while the pressure and elemental chemical composition are constant throughout the cross section under study. In the experiment, spectroscopy measurements were taken at two mutually perpendicular directions. For illustration, a numerical model of tomographic temperature field reconstruction is developed using an absorption laser spectrograph in a volume filled with carbon dioxide. The results show that the best temperature distribution reconstruction is attained at a standard deviation of 0.092. The authors are grateful to O. V. Achasov, Ye. I. Lavinskaya, and N. A. Fomin for making available the CO_2 absorptance calculation program. Figures 2; references 8.

Spatial Distribution of Plasma Parameters in Vicinity of Shock Front in Gas Discharge

927J0011A Moscow TEPLOFIZIKA VYSOKIKH TEMPERATUR in Russian Vol 29 No 1, Jan-Feb 91 pp 15-20

[Article by G. V. Naydis, Institute of High Temperatures, USSR Academy of Sciences]

UDC 533.9

[Abstract] Propagation of a shock wave through a plasma of a longitudinal discharge in an either electropositive or electronegative gas is analyzed, of concern were the distributions of charged particles and of electric field intensity on both sides of the shock front. The system of four differential equations for electrons, positive ions, negative ions, and electric field intensity in terms of their longitudinal gradients $d(n_e v_e)/dx$, $d(n_+ v_+)/dx$, $d(n_- v_-)/dx$, and dE/dx respectively ($n_{e,+,-}$ - concentrations of particles, $v_{e,+,-}$ - velocities of particles) is formulated on the assumption that the current density does not vary in time, which requires a sufficiently high ballast resistance in the external circuit. While $dE/dx = 4\pi e(n_+)$ (e - electron charge), the other three gradients involve ionization and attachment frequencies $\nu_{i,a}$ multiplied by electron-ion and ion-ion recombination coefficients $\beta_{ei,ii}$. The gas velocity V is assumed to be much lower than the velocity of electrons v_e, the gas flowing in the positive direction when it flows from anode to cathode and the shock wave propagates correspondingly from cathode to anode. Negative charges move with the shock wave and positive charges move with the gas stream. The three equations $d(n_{e,+,-}v_{e,+,-})/dx$ follows the continuity equation for the current density $dj/dx = ed(n_e v_e + n_- v_- + n_+ v_+) = 0$. The complete system of equations, valid everywhere except within a thin layer at the shock front, can be solved analytically for those distributions in (yz) planes as functions of time when the gas is only weakly ionized so that $\nu_a >> \beta_e n_+$. Although in real electronegative gas there usually exist several kinds of positive and negative ions with a different mobility μ each. The system of distribution equations is nevertheless solved for an electronegative gas containing only one kind of positive ion and thus in the $\mu_+ = \mu_-$ approximation, which is sufficiently accurate inasmuch as difference does not usually exceed 30 percent. In a real electropositive gas the quasi-neutrality of the plasma may become violated in the vicinity of a shock front. For such a gas the equation of ion distribuution is solved simultaneously with the Poisson equation. Figures 2; references 12.

Generation of Nonlinear Acoustic Vibrations in Stream of Nonhomogeneous Plasma. Equations for Amplitudes of Interacting Waves

927J0011A Moscow TEPLOFIZIKA VYSOKIKH TEMPERATUR in Russian Vol 29 No 1, Jan-Feb 91 pp 35-44

[Article by V. I. Komov and I. M. Rutkevich, Institute of High Temperatures, USSR Academy of Sciences]

UDC 533.915

[Abstract] Nonlinear acoustic perturbations in a nonhomogeneous plasma flowing through a channel are, upon expansion into series of two-dimensional standing acoustic waves with diverse scales of motion and with finite amplitudes, treated as sources of such waves. The spatial configuration of these waves can be determined from the eigenfunctions of the linearized spectral boundary-value problem. This method of analysis is analogous to Galerkin's method of analysis of hydrodynamic stability according to the nonlinear theory, except for nonself-adjointness of the linear spectral problem and nonorthogonality of its eigenfunctions. The method is based on the one-fluid model and the equations of magnetogas dynamics, ignoring the vortical component of the electric field and of the displacement current. A plasma is considered which flows in the x-direction through a rectangular channel whose height h(x) in the y-direction and width d(x) in the z-direction vary as functions of the longitudinal x-coordinate, in an external magnetic field oriented in the z-direction. The initial steady flow is assumed to be quasi-one-dimensional with a core region whose parameters, as well as the magnetic induction, are functions of the x-coordinate only. The parameters of acoustic vibrations are assumed to be functions of both y and x coordinates, in addition to being functions of time. Acoustic vibrations are assumed to separate from vortical and entropy perturbations so that their natural modes can be calculated analytically in the Wentzel-Kramers-Brillouin approximation, their characteristic frequencies, moreover, assumed to be sufficiently high. A system of equations of nonlinear acoustics in a flowing plasma is formulated, to describe superposition of nonsteady two-dimensional perturbations on a steady quasi-one-dimensional plasma flow in such a channel. It is formulated in the quadratic and thus "hydrodynamic" approximation, quadratic terms having been included and all higher-degree terms discarded in the equations of two-dimensional acoustic perturbations. Expansion of these perturbations by Galerkin's method then leads to an infinite system of equations for the amplitudes of interacting acoustic waves which includes near-resonance interaction of localized modes and is numerically solvable with any finite number of such interactions. Discarding all terms with nonzero wave vectors and then formally assuming zero amplitudes of all waves except those of three specific modes will replace this system of equations with the well known mathematical model of a resonance triplet with deviation from synchronism and thus reduce the problem to only three equations for the components of such a triplet with a certain frequency deviation. References 21.

Equations of Kinetics for Dense Gases and Liquids

927J0015A Moscow TEORETICHESKAYA I MATEMATICHESKAYA FIZIKA in Russian Vol 87 No 1, Apr 91 pp 113-129

[Article by D. N. Zubarev, V. G. Morozov, I. P. Omelyan, and M. V. Tokarchuk, Institute of Mathematics

imeni V. A. Steklov and Institute of Theoretical Physics, Statistical Physics Department in Lvov, USSR Academy of Sciences]

[Abstract] Equations of kinetics are derived for dense gases of particles whose interaction with one another can be described by the model of a solid sphere with a singular potential as well as by more realistic models. The equation of kinetics according to the revised Enskog theory is derived without additional phenomenological constraints, upon modification of the boundary condition for the Liouville equation and for the chain of Bogolyubov equations, in the approximation of "pairwise collisions" without time lag, so that correlations associated with local conservation laws with regard to momentum, total energy, and particle concentration are taken into account. Interaction of classical particles is subsequently described by a model with the short-range potential of a solid sphere and some long-range potential in the form of a smooth "tail", the border line between the two ranges not being uniquely definable and its determination thus involving an optimization process. In the limiting case of a very dense gas and absence of a long-range interparticle interaction potential, the first part of the collision integral is identical to the collision integral in the revised Enskog theory and its second part is zero. In the other limiting case of a rarefied gas and absence of the short-range solid-sphere potential the first part of the collision integral vanishes and its second part becomes identical to the collision integral in the Boltzmann equation. For the intermediate case of a small long-range Coulomb interaction potential is formulated an Enskog-Landau total bipartite collision integral which, unlike the plain Landau integral, does not diverge along small distances and whose second part is a generalization of the mean Vlasov field in the kinematic mean-field theory. Ignoring the spatial nonuniformity of the one-particle distribution function, the Enskog-Landau equation of kinetics is solved by integration with respect to cylindrical space coordinates. In the zero-order approximation with respect to gradients of hydrodynamic variables it is assumed that the one-particle distribution function is locally Maxwellian. In the first-order approximation, expressions for the stress tensor and the heat flux vector are obtained, along with expressions for the strain rate tensor, the bulk viscosity, and the shear viscosity involved in the stress tensor and for the thermal conductivity involved in the heat flux vector. The authors thank Yu. L. Klimontovich for helpful discussions and comments. Figures 1; references 25

Plasma Plunger Dynamics in Rail Mass Accelerator Channel

927J0040C Moscow TEPLOFIZIKA VYSOKIKH TEMPERATUR in Russian Vol 29 No 3, May-Jun 91 pp 446-452

[Article by A. V. Zagorskiy, S. S. Katsnelson, ITPM at the Siberian Branch of the USSR Academy of Sciences]

UDC 620.193.1:629.036.72

[Abstract] The process of electrodynamic mass acceleration (EDU) and the role of the plasma plunger decay in velocity limitations are discussed. The effect of magnetic gas dynamic factors on the plasma plunger formation and the process of momentum transfer to the accelerated body are investigated. To this end, acceleration of a dielectric body in a rail accelerator (RU) is considered and the accelerator design is examined. It is assumed that the gas dynamic parameters and current density are constant throughout the channel cross section and vary only along the longitudinal x-axis. It is also assumed that plasma initially forms as a result of an electric explosion of the shorting jumper made from the electrode material. The earlier finding that the so-called squeezed H-discharge is not realized in the rail mass accelerator and the plasma plunger has a complex extended structure is confirmed. Regular gas dynamic parameter and current density fluctuations which are directly proportionate on the current are discovered. The flow structure is shown to depend substantially on plasma's initial state. In the experiments, copper was used as the plasma-forming substance while bodies of various mass were projected in a channel with a 1 cm^2 area. Figures 7; references 15: 9 Russian, 6 Western.

Electron Spectrum and Magnetic Properties of High-T_c Superconductors as Antiferromagnetic Materials (Review)

917J0130B Kiev UKRAINSKIY FIZICHESKIY ZHURNAL in Russian Vol 36 No 6, Jun 91 pp 850-864

[Article by V. G. Baryakhtar, V. M. Loktev, Metal Physics Institute at the Ukrainian Academy of Sciences and Theoretical Physics Institute at the Ukrainian Academy of Sciences, Kiev]

UDC 537.12.67:538.945

[Abstract] Approaches to investigating the spectrum of electron and spin excitations in ordered antiferromagnetic media where mutual transformations of carriers and their transitions from one magnetic subsystem to another, or from a free one to a localized one, occur in the same way as in high-T_c superconductors (VTSP) are reviewed on the basis of numerous sources. To this end, an attempt is made to generalize the results of theoretical studies of the free carrier spectrum of HTSC. It is shown that an assumption of a strong *pd*-hybridization and possible dynamic existence of Cu^{3+} ions in the metallic HTSC phase leads to an energy band splitting into bands which become populated by carriers with the same spin direction. The magnetic susceptibility of the system is analyzed on the basis of the presence of both free and localized carriers in it and it is demonstrated that a Goldstone's spin mode determined by these carriers must exist in the high-T_c superconductor. In particular, the issues of Hamiltonian and hole spectrum, the hole interaction with spin excitations and the magnetic susceptibility of the system, and the possibility of magnon twinning in high-T_c superconductors are addressed. In all, the approaches meet basic requirements imposed by P. Anderson on the theory of HTSC magnetic and electric properties. It is shown that in the framework of a quite simple physical approach, it is possible to find a formalism which probably adequately describes real systems and makes it possible to examine the properties of both normal (including dielectric) and superconducting (SP) HTSC phases. The authors are grateful to Yu. B. Gaydidey, S. M. Ryabchenko, and S. K. Tolpygo for useful discussions of a number of topics. References 46: 14 Russian, 32 Western.

Characteristics of Resistive State of Y-Ba-Cu-O Films in Magnetic Field

917J0133A Kharkov FIZIKA NIZKIKH TEMPERATUR in Russian Vol 17 No 4, Apr 91 pp 467-475

[Article by V. G. Prokhorov, A. L. Kasatkin, G. G. Kaminskiy, M. A. Kuznetsov, V. I. Matsuy, and V. M. Pan, Institute of Metal Physics, UkSSR Academy of Sciences, Kiev]

UDC 538.22

[Abstract] An experimental study of epitaxial $YBa_2Cu_3O_{7-d}$ films in a magnetic field normal to their (a,b) plane was made, of interest being the dependence of their transition from superconducting to resistive (normal) state on the intensity of such a magnetic field. Films of this material, 200-300 nm thick and 50-100 μm wide with grains measuring about 50-100 nm along the c-axis and about 500 nm in the (a,b) plane, were deposited with a laser beam on $SrTiO_3$ substrates. Their critical temperature varied over the $T_c \approx 93$-89 K range with $\Delta T_c = 1.0$-1.5 K wide fluctuations. Their residual electrical resistivity ρ_0 varied over the 100-200 μohm.cm range, with a $\gamma = \rho_{300K}/\rho_0 = 3$ ratio of normal (300 K) to residual. Their current-voltage characteristics were measured by the pulse method so as to minimize Joule-effect heating, with current pulses applied at a repetition rate which ensured maintenance of a stable overall heat balance and readings of the voltage drop taken synchronously within the duration of pulses. These measurements were made at various levels of magnetic induction covering the B = 0-3.0 T range. The data have been processed so as to reveal the temperature dependence and the field dependence of not only the current-voltage characteristic $E = f(I)$ and its first derivative $\delta \log E/\delta I = f(I)$ but also of the pinning body force $F_p = I_c B$ and of the specific pinning force f_p. As the magnetic induction B was increased from zero up, the electrical resistivity of such films ρ_f increased first nonlinearly as $B^{1/2}$ rather than linearly according to the Bardeen-Stefan theory and then continued to increase linearly. The electric field intensity E at a constant temperature in a constant magnetic field increased first nonlinearly with the current, nearly according to the model of heat-activated flux creep, as the current was increased from zero to within the range of the critical current I_c. It then continued to increase linearly with the current so that $E = (I - I_c)\rho_f$, as the current was increased further above that I_c level. As the critical temperature was approached within the $T \approx (0.9\text{-}1.0)T_c$ range, the specific pinning force was found to vary as $(1 - T/T_c)^{5/2}$. An analysis of the results, in the approximation of a microscopically homogeneous superconductor material, indicates that the behavior of these high-T_c films in their dynamic mixed state close to the critical temperature is largely determined by the spatial nonuniformity of the order parameter and the consequent formation of one-dimensional "easy slip" vortex channels at grain boundaries (plane defects). When the Lorentz force drives the vortices through such channels across grain boundaries, then the latter become pinning centers. When the Lorentz force drives them through such channels along grain boundaries, then the field dependence of the electrical resistivity $\rho_f(B)$ appears to be analogous to that according to the Bardeen-Stefan model. The transition to a linear dependence in strong magnetic fields can be interpreted as erasure of superconductivity in those "easy slip" channels and attendant viscous vortex flow between them. The authors thank S. V. Gaponov for supplying the high-quality Y-Ba-Cu-O films. Figures 5; references 21.

Diamagnetic Properties of and Critical Currents for $Bi_{2-x}Pb_xSr_2Ca_2Cu_3O_y$ Superconductor Ceramics

917J0133B Kharkov FIZIKA NIZKIKH TEMPERATUR in Russian Vol 17 No 4, Apr 91 pp 481-491

[Article by A. M. Dolgin, I. F. Kislyak, and V. I. Donetsko, Institute of Low-Temperature Physics, UkSSR Academy of Sciences, Kharkov, I. F. Kononyuk and L. F. Makhnach, Institute of General and Inorganic Chemistry, BSSR Academy of Sciences, Minsk]

UDC 538.945

[Abstract] An experimental study of ceramic high-T_c superconductor materials $Bi_{2-x}Pb_xSr_2Ca_2Cu_3O_y$ with x = 0.2-0.6 was made for a 2-fold purpose. The first object was to determine the temperature dependence and the field dependence of their complex dynamic magnetic susceptibility $\chi = \chi' + i\chi''$ and of the critical superconducting transition temperature T_c, also the temperature dependence of their electrical resistivity ρ (ohm.cm) and of the critical current j_c (A/cm^2). The second object was to determine the dependence of T_c, j_c, and ρ_n (electrical resistivity in normal state) on the Pb content. Ceramic rectangular 15 mm long bar specimens (1.5 mm thick, 5 mm wide) specimens of these materials with x = 0.2, 0.3, 0.4, 0.5, and 0.6 were produced from $Sr(NO_3)_2$, $Ca(NO_3)_2$, Bi_2O_3, Pb_3O_4, and CuO mixtures by firing at a temperature within 1115-1130 K and holding for about 300 h. Those with x = 0.2-0.4 were almost pure 2223-phase solid solutions, as indicated by x-ray diffractograms, a small amount of Ca_2PbO_4 appearing as a new phase in the x = 0.5 ceramic and a larger amount of it present in in the x = 0.6 ceramic. Measurements were made in a longitudinal magnetic field alternating at a frequency f = 1 kHz, as did the magnetic induction $B = B_0 \sin 2\pi f$ with a constant amplitude B_0 = 0.03 mT for $\chi(T)$ measurements and with the amplitude varied over the 0.03-2.0 mT range for $\chi(B)$ measurements. The electrical resistance was measured by the standard current-voltage method with the current varied over 0.1-0.25 A/cm^2 range. The critical current was determined on the basis of a E = 5 μV/cm electric field intensity. The temperature dependence of χ', χ'' (real and imaginary parts of magnetic susceptibility), and the electrical resistivity ρ was determined on the basis of measurements made while the specimens were cooled at a rate of about 0.5 K/min. The field dependence of χ', χ'', and the critical current j_c at the T = 77.4 K temperature was determined on the basis of measurements made with the specimens held in liquid nitrogen while the magnetic induction was varied linearly from B = 0 to $B_{max} \simeq 80$ mT and back to B = 0 at a rate of 0.1 mT/s. An analysis of the results reveals a behavior of these ceramics consistent with the granular weak-link superconductor model. The field dependence of χ', χ'', and the critical current j_c at 77.4 K is characterized by a large hysteresis, evidently the effect of local magnetic fields superposing on the external magnetic field and the magnetic fields of captured flux in the weak-link regions. The temperature dependence of the critical current indicates that the latter varies approximately according to the $j_c = j_{c0}(T_{cj} - T)^{1.4}$ relation characteristic of Josephson media, particularly those with SNIS junctions, in the $j_c \leq j_c^b$ range and approximately according to the $j_c = j_{c0}\exp(-T/T_0)$ relation characteristic of single crystals in the $j_c > j_c^b$ range. In these relations T_{cj} denotes the upper phase coherence temperature, j_{c0} denotes the induction-dependent critical current for individual grains, j_c^b denotes a corner level of the critical current density, approximately 5 A/cm^2, and T_0 denotes the apparent zero-resistivity temperature. With the aid of these data, it is thus possible to separate intragranular and intergranular processes. The data reveal, moreover, that replacement of Bi with Pb alters the characteristics of intergranular junctions but does not influence the properties of the 2223-phase bulk superconductor. Figures 8; tables 1; references 14.

Current-Voltage Characteristics of High-T_c Superconductors Containing Thallium

917J0133C Kharkov FIZIKA NIZKIKH TEMPERATUR in Russian Vol 17 No 4, Apr 91 pp 492-497

[Article by V. I. Trefilov, I. S. Shchetkin, T. Sh. Osmanov, and N. V. Abramov, Institute of Problems in Materials Science, UkSSR Academy of Sciences, Kiev]

UDC 538.945

[Abstract] An experimental study of ceramic $Tl_2Ba_2Ca_2Cu_3O_x$ superconductors was made concerning the temperature dependence of their current-voltage characteristics and critical current. Microbridges 20-50 μm wide were formed on ceramic bricks and on 0.03-0.07 mm thick films which, mixed with an organic binder, had been pasted over (2-10) x (1.5-4) mm^2 large surface areas on various substrates. The effective cross-section area S^* of the microbridges on bricks varied from 10^{-6} cm^2 to 10^{-3} cm^2 orders of magnitude. Superconducting transition of the thick-film coatings was completed at a temperature T_c^0 within 100-90 K on plates of aluminum alloys, within 105-90 K on Policor plates, within 106-90 K on silver wires, within 106-94 K on wires of nonprecious metal alloys, within 116-110 K on sapphire plates, within 122-118 K on plates of MgO single crystals, and at 125 K on ceramic bricks. The current and voltage measurements were made inside a thermostat with temperature regulation down to 77.8 K, a cryostat with liquid nitrogen being included as well as means for prevention of temperature drift and Joule-effect heating. The current-voltage characteristic of most microbridges, whether on ceramic bricks or on thick-films, include a voltage dip in the low-current range and voltage steps in the high-current range. The dip is sharp at 77.8 K, becomes flatter or changes into a kink while it shifts toward lower currents at higher temperatures, and vanishes at the T_c^0 temperature. The voltage steps are

steepest on the current-voltage characteristics of microbridges with the smallest effective area. There are only one or two of them at 77.8 K, more of them appearing and their slopes becoming milder at higher temperatures. The dip is hypothetically associated with the narrower energy gap of these two-gap Tl-ceramic superconductors, whose transition to the normal state is completed when the wider energy gap vanishes as the current becomes sufficiently high for the voltage to continue to steeply increase. The temperature dependence of both energy gaps is, moreover, analogous to that in the Bardeen-Cooper-Schrieffer theory. The hypothesis regarding the voltage dip is further supported by the temperature dependence of the critical current, the latter having been found to decrease monotonically from 6 kA/mm^2 at $0.6T_c$ to zero at T_c along approximately the same concave curve for all microbridges. Such a trend of the temperature dependence of the critical current indicates a laminar structure of these Tl-ceramic superconductors. The authors thank members of the Institute of Low-Temperature Engineering Physics at the UkSSR Academy of Sciences for discussing the results of this study. Figures 3; references 16.

Spectroscopy of $GdBa_2Cu_3O_{7-x}$ Superconductor Films

927J0002 Kiev UKRAINSKIY FIZICHESKIY ZHURNAL in Russian Vol 36 No 7, Jul 91 pp 1099-1103

[Article by V. G. Litovchenko, S. I. Frolov, V. I. Gavrilenko, and Ksiong Guang Cheng, Institute of Semiconductors, UkSSR Academy of Sciences, Kiev]

UDC 546.562:538.958

[Abstract] An experimental study of epitaxial $GdBa_2Cu_3O_{7-x}$ superconductor films was made, such films having been deposited on $SrTiO_3$ substrates with a structurally homogeneous mirror surface. Films of this superconductor material are known to be more stable in air than films other high-T_c superconductor materials such as $YBa_2Cu_3O_{7-x}$, $ErBa_2Cu_3O_{7-x}$, $TmBa_2Cu_3O_{7-x}$, inasmuch as gadolinium inhibits oxidation and therefore degradation of the material. Two specimens were tested, their critical superconducting transition temperature T_c being 89.1 K and 87.7 K respectively. Structural examination of these films was done in an x-ray diffractometer with a KCu_α-radiation source. Their diffraction spectra contained peaks characteristic of an orthorhombic structure with the c-axis perpendicular to the film surface, the small angle Γ indicating a high degree of structural perfection. The spectral characteristic of the imaginary part of their pseudodielectric permittivity ε_2 was established by photometric spectrum ellipsometry with a rotating analyzer, in a geometry with the c-axis of the films in the plane of radiation incidence. These measurements have revealed a mild rise of ε_2 over the 2.5-2.8 eV range and two sharp peaks: one at approximately 3.8 eV, one at approximately 4.3 eV. On that basis the Grueneisen gamma Γ and the characteristic relaxation time τ have been calculated, the former found to increase and the latter found to decrease with increasing concentration of free charge carriers. The chemical composition of both films was evidently almost stoichiometric, with $x \cong 0.14$ ($T_c = 89.1$ K) and $x \cong 0.11$ ($T_c = 87.7$ K) respectively. The two peaks in the ε_2-spectra are attributable to interband transitions $1 \rightarrow 4$ (electric field perpendicular to c-axis) and $2 \rightarrow 4$, $3 \rightarrow 5$ (electric field parallel to c-axis). Figures 2; tables 2; references 8.

Ferroelasticity of Twin Structure of 123-Phase High-T_c Superconductors

927J0002B Kiev UKRAINSKIY FIZICHESKIY ZHURNAL in Russian Vol 36 No 7, Jul 91 pp 1111-1115

[Article by V. S. Nikolayev, Institute of Theoretical Physics, UkSSR Academy of Sciences, Kiev]

UDC 537.312.62

[Abstract] The pressure dependence of the structural parameters of twin crystals of nonstoichiometric 123-phase superconductor compounds such as $YBa_2Cu_3O_{7-d}$ with $d << 1$ is analyzed theoretically on the basis of the Frenkel-Kontorova twinning model (Yu. B. Gaydidey V. M. Loktev, and V. S. Nikolayev, SOLID-STATE COMMUNICATIONS Vol 75 No 6, 1990), considering that $Cu(1)^{2+}$ - O^{2-} interaction is the principal mechanism of twin formation under a uniaxial pressure and assuming that the "competing" O-O interaction has a harmonic potential. This model, unlike the classical ferroelastic model involving the standard Ginzburg-Landau functional with an order parameter proportional to the strain, takes into account nonstoichiometry and does not assume a so far unconfirmed dependence of the twinning space period on the size of grains (single crystals) in the superconductor ceramic. It furthermore takes into account not only nonstoichiometry of the chemical composition but also redistribution of the oxygen atoms among vacancies and deformation of the crystal lattice in the twinning process. A second order parameter $\varepsilon = (\varepsilon_{11} - \varepsilon_{22})/2^{1/2}$ (ε_{ij} - strain tensor) which characterizes rhombic transformation from square to rectangle is introduced and the Hamiltonian representing the total energy is supplemented accordingly so as to include the surface energy of a periodic structure. The total energy then has a minimum, expressions for the minimum total energy and for the corresponding order parameter ε being readily obtained by differentiation. These expressions indicate a dependence of the twin deformation on the displacement of O-ions from their equilibrium positions, as it does on the Cu-O interaction, and describe ferroelastic effects such as vanishing of the twin structure when the uniaxial internal pressure exceeds its critical level. The author thanks participants of the seminar chaired by A. S. Davydov for helpful discussions, also Yu. B. Gaydidey and V. M. Loktev for support.

Possibility of Controlling Velocity of Solitary Acousto-Electromagnetic Waves in Crystals With Quadratic Electrostriction

927J0002C Kiev UKRAINSKIY FIZICHESKIY ZHURNAL in Russian Vol 36 No 7, Jul 91 pp 1095-1099

[Article by O. N. Bulanchuk and G. N. Burlak, Kiev University imeni T. G. Shevchenko]

UDC 534:621.382:534:535

[Abstract] Considering that a solitary acousto-electromagnetic envelope wave can form in crystals with nonlinear electrostriction, the dependence of its velocity on the amplitude of the incident pump wave is shown to make it possible to control its velocity by amplitude modulation of that incident pump wave. This is demonstrated on a crystal of the 3m point group ($LiNbO_3$, $BaTiO_3$) at a temperature below -90°C pumped by a laser along its x-axis, nonlinear interaction of waves then propagating in this direction being strongest when the frequencies and the wave numbers of the two ordinary and extraordinary electromagnetic waves ($\omega_{o,e}$, $k_{o,e}$ as well as those of the transverse acoustic wave (Ω_a), degenerate case of two acoustic waves having the same frequency and wave number) satisfy the conditions of phase synchronism. Theoretical analysis of their interaction is based on the system of three dimensionless partial differential equations in the approximation of slowly varying amplitudes, assuming a constant relative phase of waves ψ = difference $-\psi_o + \psi_e + 2\psi_a + \delta kx = \pi/2$ ($\delta k << k_{o,e}$). As two examples of acoustic signal envelopes are considered one with an initial Lorentz pulse and one with a hyperbolic "priming" pulse. Numerical analysis and calculations confirm that the velocity of solitary envelopes of sufficiently wide acoustic pulses propagating through nonlinear crystals can be widely controlled by amplitude modulation of the incident electromagnetic wave (laser radiation), even being possible to stop them and to reverse the direction of their propagation. Figures 3; references 5.

Microwave Absorption by Single Crystals of High-T_c Superconductor in Weak Magnetic Fields

927J0003A Moscow DOKLADY AKADEMII NAUK SSSR in Russian Vol 317 No 2, Mar 91 pp 344-347

[Article by V. I. Muromtsev, V. V. Troitskiy, I. O. Maslennikov, M. A. Krykin, and A. A. Bush, Scientific Research Institute of Physical Chemistry imeni L. Ya. Karpov, Moscow]

UDC 537.312.62

[Abstract] An experimental study of microwave absorption by single crystals of the $GdBa_2Cu_3O_7$ high-T_c superconductor material at temperatures below critical (T_c = 63 K) in weak magnetic fields of not higher than 1 Oe intensity. Measurements were made with an Electron-Paramagnetic-Resonance microwave superheterodyne spectrometer operating in the 3 cm band and a pair of Helmholtz coils instead of an electromagnet scanning the magnetic field. These two coils were spaced in quadrature around a cylindrical H_{011}-mode resonator cavity and the entire structure was placed inside a can made of the magnetically soft 20Fe + 80Ni:(Cr,Si) alloy, shielding it so effectively from the terrestrial and stray magnetic fields that the the residual "null" magnetic field intensity inside did not exceed 100 mOe. Specimens of $GdBa_2Cu_3O_7$ single crystals were prepared in the form of 0.1 mm thick 1 mm square plates with the c-axis normal to their two parallel faces. Such a crystal was placed inside the resonator cavity with the c-axis parallel to the H_1 microwave field and rotated by a goniometer about this axis, such a configuration ensuring maximum absorption of incident microwave power. A helium cryostat was attached to the spectrometer for cooling a crystal from 300 K stepwise down to 3.8 K with precise temperature stabilization, within +/-0.1 K at each level, cooling being done with a crystal in the residual "null" magnetic field only. The power of incident microwave radiation was varied from 50 mW to 0.5 kW (0-80 dB) with and without amplitude modulation of the H_0 microwave field. Modulation was effected by passage of an electric current alternating at a frequency of 500 kHz through two pairs of rods forming two loops inside the resonator cavity parallel to its axis, the amplitude of modulation being varied over the low 0.1-10 mOe range. The microwave absorption spectrum was found to contain different series of narrow lines depending on the intensity of the incident microwave H_1 field and on the temperature. The minimum spectral field period, smallest field separation ΔH_0 between these lines in that spectrum, did not depend on the temperature when the microwave power was raised from 50 mW by 60 dB but did depend on the temperature in an inverse relation when the microwave power was pulled back down by 45 dB. Two series of lines were found to coexist in the absorption spectrum, one and the same series appearing and vanishing periodically with respect to the H_1 microwave field. The microwave absorption spectrum of such superconductor crystals in a weak magnetic field thus appears to be highly sensitive to changes in the intensity of that field. The sensitivity of that spectral field period to temperature changes below critical may refute the now most widely accepted hypothesis that natural weak links exist and form Josephson junctions in single crystals of such a high-T_c superconductor, the periodic fine structure of the microwave absorption spectrum having been heretofore associated with changes in the fluxoidal state during transitions or with macroscopic quantum interference and having been based on earlier experimental evidence indicating temperature independence of that spectral field period. Article presented by Academician Ya. M. Kolotyrkin on 6 December 1990. Figures 3; references 9.

Structure of Epitaxial $YBa_2Cu_3O_{7-d}$ Films

927J0005 Moscow FIZIKA TVERDOGO TELA in Russian Vol 33 No 1, Jan 91 pp 25-29

[Article by A. L. Vasilyev, S. I. Krasnosvobodtsev, V. P. Martovitskiy, Ye. V. Pechen, and V. V. Rodin, Institute of Physics imeni P. N. Lebedev, Moscow]

UDC 536.312.62

[Abstract] A structural examination of $YBa_2Cu_3O_{7-d}$ grown on $SrTiO_3$ and MgO single crystals by two methods was performed, some films having been deposited on each substrate at rates of 0.5-4 nm/s by pulsed laser-beam vaporization of two targets and some films having been deposited on each substrate at rates of 0.1-0.3 nm/s by magnetron sputtering with a direct current. The optimum substrate temperature for deposition of films with a stoichiometric Y-Ba-Cu composition by both methods was within the 690-740°C range. The optimum oxygen pressure for laser beam vaporization and the optimum oxygen or oxygen+argon pressure for magnetron sputtering was about 1 torr. Formation of large clusters during laser beam vaporization was prevented by orienting the two plasma streams from the two targets so as to make them collide. The chamber for magnetron sputtering had been constructed so as to minimize bombardment of the rising film surface by negative oxygen ions and atomized particles. Structural examination was performed in a DRON-2.0 x-ray diffractometer with a CuK_{α}-radiation source and a bent graphite monochromator, an extra slit for passage of local reflexes facing a film specimen, and also under a Phillips EM-430ST transmission electron microscope in the axial illumination mode with 250 kV and 300 kV accelerating voltages. For films on (001) $SrTiO_3$ substrates the critical superconducting transition temperature varied from 92.0 K to 90.5 K and the transition range was not wider than 0.5 K, based on electrical resistance and magnetic susceptance measurements, their electrical resistivity at 100 K varying over the 40-60 μohm.cm range and the critical current at 77 K being higher than 5 MA/cm^2. For films on (100) MgO substrates the critical superconducting temperature varied from 90 K to 89 K and the transition range was not wider than 1 K. Analysis of the x-ray diffractograms revealed an adverse influence of high-energy atomized particles on the film structurization, their presence causing formation of at least some directionally disordered 123-phase even on (100) $SrTiO_3$ substrates, raising the the oxygen pressure above the optimum level not helping and only appreciably slowing down the deposition process. Lowering the oxygen pressure lowered the critical superconducting transition temperature and somewhat widened the transition range. All films, essentially single crystals, were found to include transposition twins. The results of this study indicate that it is feasible to grow epitaxial $YBa_2Cu_3O_{7-d}$ single-crystal on hot substrates of both kinds with adequate thermalization of high-energy atomized particles under optimum oxygen pressure and to thus produce, without subsequent annealing, epitaxial films with a degree of structural perfection determined solely by the degree of perfection of the substrate structure. Figures 5; references 5.

Dependence of Properties of Y-Ba-Cu-O Ceramics on Their Structure

927J0005B Leningrad FIZIKA TVERDOGO TELA in Russian Vol 33 No 1, Jan 91 pp 166-173

[Article by T. S. Orlova, N. N. Peschanskaya, L. K. Markov, B. I. Smirnov, and V. V. Shpeyzman, Institute of Engineering Physics imeni A. F. Ioffe, USSR Academy of Sciences, Leningrad, J. Engert and H.-J. Kaufmann, Laboratory of Low-Temperature Physics at GDR Academy of Sciences, Berlin, U. Schlaefer and L. Schneider, Institute of Solid-State Physics, GDR Academy of Sciences, Dresden]

UDC 537.312.62

[Abstract] An experimental study of $YBa_2Cu_3O_{7-d}$ ceramics was made, three groups of specimens each having been produced by a different method but all having an exactly stoichiometric Y-Ba-Cu composition. All specimens were produced from the same batch of thoroughly mixed Y_2, $BaCO_3$, and CuO powders of 4 μm, 5 μm, and 6 μm grain size respectively. The mixture was compacted and sintered at 1208 K in air for 15 h, then cooled for 14 h at a rate gradually decreasing from 150 K/h to 45 K/h. The oxygen content necessary for a stoichiometric Y-Ba-Cu composition was ensured by subsequent annealing at 673 K in pure oxygen for 10 h. Specimens "A" were not further treated. Their characteristics were: average grain size 10 μm, density 4.79 g/cm^3, modulus of elasticity 76.5 GPa, and critical superconducting transition temperature T_{c0} = 89 K. Specimens "B" were pulverized in a rotary mill to a 15 μm average grain size and then reprocessed as before. Their final characteristics were: average grain size 30 μm, density 5.64 g/mg, modulus of elasticity 92.0 GPa, and critical superconducting transition temperature T_{c0} = 85.5 K. Specimens "C" were pulverized to 15 μm average grain size and reprocessed as before, then pulverized again in a ball mill to 5 μm average grain size and reprocessed as before. Their final characteristics were: average grain size 15 μm, density 5.64 g/cm^3, modulus of elasticity 100.3 GPa, and critical superconducting transition temperature T_{c0} = 86 K. All specimens were those of the 123-phase, with only a slight excess of CuO in some. Specimens "B" were of the widest grain size fraction and theirs was the widest range of superconducting transition, $\Delta T_c \approx 4$ K, evidently owing to the highest level of internal stresses and structural defectiveness. All specimens were tested for the role of internal stresses and for the temperature dependence of the rate of inelastic strain over the 300-77 K temperature range, a correlation between the structure and superconducting transition of $YBa_2Cu_3O_{7-d}$ ceramics having been established on the basis of measurements. Their current-voltage characteristics and critical current were measured without a magnetic field and then in magnetic

fields of 25 Oe and 50 Oe intensity, in each case under no load and under compressive loads of 25 MPa and 50 MPa. The results indicate a sensitivity of the critical current to both a magnetic field and a compressive load, most sensitive to change in the magnetic field but least sensitive to change in the compressive stress being the critical current for "B" ceramic and most sensitive to change in the compressive stress but least sensitive to change in the magnetic field being the critical current for "C" ceramic. Figures 6; tables 3; references 13.

Long-Wavelength Infrared Radiation Spectra of $Bi_2Sr_2Ca_{0.6}Ba_{0.4}Cu_{1.9}O_x$ in Vitreous and Crystalline (Superconducting) States

927J0005C Leningrad FIZIKA TVERDOGO TELA in Russian Vol 33 No 1, Jan 91 pp 182-186

[Article by V. A. Ryzhov. V. A. Bershteyn, B. T. Melekh, and Yu. N. Filin, Institute of Engineering Physics imeni A. F. Ioffe, USSR Academy of Sciences, Leningrad]

UDC 537.312.62

[Abstract] In an experimental study of vitreous and polycrystalline $Bi_2Sr_2Ca_{0.6}Ba_{0.4}Cu_{1.9}O_x$ the long-wave infrared radiation spectra of this material in both states were measured at temperatures including the 80 K critical superconducting transition temperature for the crystalline material, for a comparison of these spectra with those superconducting orthorhombic and nonsuperconducting tetragonal $YBa_2Cu_3O_{7-d}$. The reflection spectra were measured in a Hitachi FIS-21 long-wave spectrometer with an attachment for a 10° angle of incidence, an aluminum mirror serving as a 100 percent reflection standard. Transmission spectra were measured at temperatures from 296 K down to 80 K for tracking superconducting transition and attendant changes, reflection spectra at low temperatures not being measurable with that attachment. The spectra indicate a "softening" of flexural vibration modes of the Cu-O bonds in Cu-O planes during superconducting transition, this effect being evidently characteristic of all CuO-based superconductor materials. The spectra of polycrystalline $Bi_2Sr_2Ca_{0.6}Ba_{0.4}Cu_{19}O_x$ that it absorbs $\nu > 170$ cm^{-1} radiation more intensely at 80 K than at 296 K and absorbs $\nu < 170$ cm^{-1} radiation less intensely at 80 K than at 296 K. This intersection of spectra is consistent with the Bardeen-Cooper-Schrieffer theory and attributable to manifestation of an energy gap, the crossover frequency $\nu = 170$ cm^{-1} corresponding to an energy gap $2\Delta \approx 3kT_c$ only slightly smaller than the theoretically predicted $3.5kT_c$. Figures 3; references 21.

Detecting Optical Radiation With Bi-Sr-Ca-Cu-O High-T_c Superconductor Films

927J0005D Leningrad FIZIKA TVERDOGO TELA in Russian Vol 33 No 1, Jan 91 pp 41-54

[Article by Yu. A. Kumzerov, M. Ye. Leshchenko, S. G. Romanov, and A. V. Suvorov, Institute of Engineering Physics imeni A. F. Ioffe, USSR Academy of Sciences, Leningrad]

UDC 537.312.62

[Abstract] An experiment was performed with 2212-phase Bi-Sr-Ca-Cu-O high-T_c superconductor films as detectors of optical radiation, such 0.3-0.9 μm thick films having been deposited on polycrystalline MgO substrates by ion-beam sputtering of a $BiSrCaCu_2O$ target and then annealed in an oxygen stream to a 90 percent 2212-phase composition. Their superconducting transition extended over a wide temperature range, from 90 K to 60 K. On these films were deposited four gold tabs for measurement of their current-voltage characteristics in the current-source mode at 77 K and 4.2 K temperatures. A light-emitting diode directly above the film served as source of 800 nm radiation. A wire loop surrounding the film and loading a coaxial feeder was provided for simultaneous application of a microwave field, its frequency being adjustable over the 0.5-10 GHz range. A solenoid surrounding the film was provided for application of an external magnetic field perpendicular to the conduction current. The two voltage signals ΔV_{opt} and ΔV_{mw} representing respectively distortion of the current-voltage characteristics by optical radiation and by microwave radiation were measured by the standard modulation method, with 100 percent modulation of the light intensity by application of 8 kHz voltage pulses to the diode and with 50 percent amplitude modulation of the microwave signal by a sinusoidal signal of that same frequency. The fine structure of the current-voltage characteristics was analyzed by way of analog differentiation, the voltages V_ω and $V_{2\omega}$ proportional respectively to the first derivative and the second derivative of the current-voltage curve being measured while the displacement current was modulated by small audio-frequency signal. The current-voltage characteristics of these films were found to be analogous to those of a Josephson junction, with fluctuations taken into account. A magnetic field and microwave radiation suppressed superconductivity, while optical radiation enhanced it by lowering the electrical resistance of weak links. This latter effect cannot be attributed to photoconduction, however, because it has been observed only during superconducting transition and also because these high-T_c materials contain no semiconductor phases as indicated by the metal-like temperature dependence of their electrical resistance. Rather, this effect is similar to microwave-stimulated superconductivity. The results of this experiment confirm the feasibility of using such films with granular structure for wideband detectors of video signals, weak intergranular bonds playing the principal role in the detection of optical radiation. Figures 6; references 9.

Possible Nature of High-Temperature ($T_c \approx 200$ K) Superconductivity of Copper Oxide CuO_{1-x}

927J0009A Leningrad PISMA V ZHURNAL TEKHNICHESKOY FIZIKI in Russian Vol 17 No 7, 12 Apr 91 pp 1-3

[Article by M. V. Krasinkova and B. Ya. Moyzhes]

[Abstract] In a recent experiment (C. B. Azzoni et al.: ZEITSCHRIFT d. NATURFORSCHUNG Vol 45a No 6, 1990) pure CuO_{1-x} ceramic produced by calcination of polycrystalline copper oxide in a nitrogen atmosphere and consisting of two phases CuO + Cu_2O was found to become superconducting during transition with the critical temperature within the 200-230 K range and with the electrical resistance in this state approximately 11 orders of magnitude lower than in the normal state. This superconductivity, originally thought to be a filamentary or surface phenomenon, seems to confirm the hypothesis that formation of a thin epitaxial CuO layer with a cubic rather than monoclinic crystal structure (M. V. Krasinkova and B. Ya. Moyzhes: FIZIKA TVERDOGO TELA Vol 32 No 10, 1990) on the surface of the Cu_2O phase with a b.c.c. crystal lattice is responsible for such a high critical superconducting transition temperature. Figures 1; references 9.

Modification of High-T_c Superconductor Film Surface by High-Intensity Pulse of Vacuum Ultraviolet Radiation

927J0012A Moscow DOKLADY AKADEMII NAUK SSSR in Russian Vol 318 No 6, Jun 91 pp 1377-1380

[Article by Yu. V. Afanasyev, V. A. Veretennikov, D. G. Yemelyanenkov, V. I. Yepikhin, A. P. Kanavin, O. G. Semenov, A. A. Mazayev, and V. I. Makhov, Institute of Physics imeni P. N. Lebedev, USSR Academy of Sciences, Moscow]

UDC 621.36.403

[Abstract] Polishing the surfaces of high-T_c superconductor films by treatment with vacuum ultraviolet radiation was studied experimentally, a micropinch serving as source of this radiation and of soft x-rays as well as of a plasma stream. A dense hot plasma was formed by pinching the channel of a high-current (150 kA) discharge between copper electrodes in the vapor of their erosion products. This plasma in turn generated vacuum ultraviolet radiation and soft x-rays in pulses of E = 50 J energy and $\tau \approx 100$ ns duration, the maximum energy within their spectrum falling within the 50 eV band. Superconductor films were produced by magnetron sputtering of stoichiometric Y-Ba-Cu-O targets with a direct current onto sapphire substrates, over 0.1 μm thick SiO:Y stabilized interlayers. Subsequent annealing at 820-860°C ensured formation of the orthorhombic phase, its superconducting transition beginning at 90 K and ending at 82-72 K. The critical current at 77 K did not exceed 1 kA/cm^2. These films were placed in cassettes and exposed to radiation from a source under high vacuum successively 60 mm, 100 mm, and 150 mm away from them. Use of copper electrode minimized contamination of the film surface by the impinging plasma. The films were thus treated with 10-100 pulses. A film surface 100 mm away from the radiation source was found to have begun smoothing out after 10 pulses and its roughness to have been reduced to 0.1 gmm asperity height after 50 pulses without an appreciable change of electrophysical properties, except for an about 15 percent change in the electrical surface resistance. The electrical surface resistance of films 60 mm away from the radiation source had increased by a factor of 5 after two pulses and by a factor greater than 100 after 10-50 pulses, indicating transformation into the tetragonal phase. A theoretical analysis of the mechanisms of micropinch plasma action on the surface of such films is is based on an energy density of a plasma pulse $\varepsilon \approx 0.04$ J/cm^2 a radiation power density $q \approx \varepsilon/\tau \approx 0.4$ MW/cm^2. The film surface temperature T_0 is calculated accordingly, assuming that the surface absorbs the entire incident energy. It is found to be approximately 2000 K and thus much higher then the about 1300 K melting point of the superconductor film material. The principal surface smoothing mechanism, therefore, is formation of a liquid layer which then spreads over the surface at a rate $j = \int_0^h v(y)dy$ (y - horizontal coordinate, v - velocity of flow) by action of body forces due to capillary pressure and nonuniformity of surface tension. Assuming further that the existence of the liquid phase is sufficiently short for the relative change of thickness δh/h of the liquid layer during the mass transfer process to be very small, the number of pulses needed for effective smoothing of the film surface by reducing the height of asperities ξ is shown to depend largely on the spatial scale of these pulses as well as on their duration and energy content. From the continuity equation $\delta h/\delta t + \delta j/\delta x = 0$ follows $\delta h_n(x) = -D\delta^4\xi(x)/\delta x^4$ (n - number of incident pulses, x - vertical coordinate). It is noteworthy that, for a given number of pulses n, asperities with the transverse dimension smaller than (or equal to) approximately $(Dn)^{1/4}$ will become smooth and those with the transverse dimension larger than (or equal to) $(Dn)^{1/4}$ will remain almost undistorted. The value of coefficient D can be estimated by assuming a dynamic viscosity of 0.01 P and a surface tension of 1000 dyne/cm. Figures 1; references 6.

Influence of Fluctuations on Hall Effect and Thermomagnetic Effects in Superconductor Near Critical Temperature

927J0016C Moscow ZHURNAL EKSPERIMENTALNOY I TEORETICHESKOY FIZIKI in Russian Vol 99 No 6, Jun 91 pp 1816-1826

[Article by A. A. Varlamov and D. V. Livanov, Moscow Institute of Steel and Alloys]

[Abstract] Galvanomagnetic and thermomagnetic effects in high-T_c superconductors during superconducting transition are analyzed theoretically for the influence of superconductivity fluctuations on them in the vicinity of the critical temperature. The analysis is based on Kubo-Greenwood relations for the kinetic coefficients of electron and heat transfer in weak magnetic fields, and in a temperature field with small gradients so that the perturbation theory may be applied in its first order with respect to deviations from homogeneity of the material as well as from zero intensity of the magnetic field. Meanwhile, however, the Green's functions of an electron must take into account its interaction with a weak magnetic field. The analysis is aided by schematic diagrams, first being considered three free one-electron Green's functions (no intrinsic magnetic field) forming a loop with three vertices two of which correspond to two

flux operators while the third one represents interaction of the electron with an external constant magnetic field. Calculations are made for the model of a normal multilayer metal with the Fermi surface in the form of a corrugated cylinder. Subsequently added corrections for superconductivity fluctuations in such a material are shown to bring about anomalies in the temperature dependence of its Hall conductivity, and Nernst, Ettinghausen, Leduc-Righi coefficients, noteworthy being that all four corrections are identically temperature dependent. The authors thank A. V. Ustinov for pointing out the timeliness of this topic. References 5

Spin-Density Waves and Quantum Hall Effect in Organic Superconductors

927J0016D Moscow ZHURNAL EKSPERIMENTALNOY I TEORETICHESKOY FIZIKI in Russian Vol 99 No 6, Jun 91 pp 1849-1852

[Article by A. G. Lebed, Institute of Theoretical Physics imeni L. D. Landau, USSR Academy of Sciences]

[Abstract] Spin-density waves which a magnetic field induces in organic superconductors of the $(TMTSF)_2X$ ($X = ClO_4$, PF_4) family are considered, these spin-density waves being an analog of the two-dimensional quantum Hall effect. Equations describing the order parameter of this spin-density-wave state are obtained by expansion of the free energy in the Landau approximation, consistent with lattice symmetry in real space, at temperature $T = 0$. They are subsequently solved in the quantum limit $\omega_c >> T$ (ω_c - cyclotron frequency) for an order parameter described as a periodic function of the space coordinate and expandable into a series of plane waves. For this case, the Hall conductivity σ_{xy} is calculated, after Green's functions $G^{+/-\ +/-}(n\omega_c, p_y, p_z; x, x')$ have been averaged over fast oscillating electrons (n - order of harmonic, p - momentum) and an approximate expression for the free energy F has been obtained from the series of applicable perturbation theories. The experimentally obtained quantization of this Hall conductivity is evidently consistent with the more general Thouless-Halperin theory. The author thanks L. P. Gorkov and V. M. Yakovenko for helpful suggestions and comments. Figures 2; references 15.

Soliton Thermodynamics of Quasi-One-Dimensional Antiferromagnetics in External Magnetic Field

917J0135A Kharkov FIZIKA NIZKIKH TEMPERATUR in Russian Vol 17 No 3, Mar 91 pp 343-366

[Article by B. A. Ivanov and A. K. Kolezhuk, Institute of Metal Physics, UkSSR Academy of Sciences, Kiev]

UDC 538.22

[Abstract] Diffusion of kinks in an antiferromagnetic material in an external magnetic field is analyzed on the basis of microscopic theory, both normal diffusion with $D\eta = T$ (D - diffusion coefficient, η - viscosity coefficient, T - absolute temperature) and anomalous diffusion due to collisions without change of momentum being considered. While normal D-diffusion takes place when a small momentum is transferred at a low frequency, anomalous D^*-diffusion can be intense only when a large momentum is transferred at high frequency. An external magnetic field, inevitably attending every experiment, is shown to influence normal diffusion and the viscosity in rhombic antiferromagnetic materials such as $CsMnCl_3 \cdot 2H_2O$ crystals with an axis of easy magnetization (z) and an axis of difficult magnetization (x) or in antiferromagnetic materials such as TMMC crystals with a plane of easy magnetization. The role of anomalous diffusion cannot possibly be significant, as indicated by the form of the dynamic structural factor $S^{\alpha\beta}(q,\omega)$ (Fourier component of the spin correlation function representing the response of magnetic system to external magnetic field in the space-time domain) and particularly of its center peak. These conclusions follow from an analysis of soliton thermodynamics, taking into account the structure of moving kinks and their restructurization beginning at the critical velocity. A model is selected, a one-dimensional antiferromagnetic crystal with two sublattices. The soliton solutions to its Landau-Lifshits equations are obtained and analyzed on the basis of its free energy functional and anisotropy energy, considering three orientations of the external magnetic field: parallel to the x-axis, parallel to the y-axis and parallel to the z-axis. The effect of an external magnetic field on the thermodynamics of a soliton gas is subseqently analyzed on a phenomenological basis, specifically considering the decrease of free energy at nonzero temperatures as the number of magnons decreases upon formation of kinks and also considering that in the absence of Lorentz-invariance the spectrum of remaining magnons may depend on the velocity of these kinks. Next is analyzed Brownian motion of kinks in a thermostat, assuming absence of kink-kink interaction in a rarefied soliton gas. The contribution of each kind of kink diffusion to the dynamic structural factor is then evaluated, normal (Einstein) diffusion being shown to change it appreciably and nondissipative anomalous diffusion being shown not to influence it. Phase transitions within a kink are, moreover, shown to occur not only in an external magnetic field but also owing to energy invariants of the Dzyaloshinskiy interaction kind with a nonantisymmetric D_{ik} tensor. The authors thank V. G. Baryakhtar and A. Bishop for helpful discussions, also G. K. Oksyuk for assistance and discussions. Figures 7; references 31.

Nonequilibrium Properties of Van Vleck Paramagnetic Materials in Superconducting Tunnel Junctions

917J0135B Kharkov FIZIKA NIZKIKH TEMPERATUR in Russian, Vol 17 No 3, Mar 91 pp 382-389

[Article by A. A. Kosov, Kazan State University imeni V. I. Ulyanov-Lenin]

UDC 538.945

[Abstract] The behavior rare-earth impurity ions in superconducting electrodes of tunnel junctions is analyzed, considering their Van Vleck paramagnetism and the direct relation between the population of their energy levels and various measurable properties such as width and shift of the NMR (nuclear-magnetic resonance) lines and cross-section for inelastic neutron scattering. Because the parameters of their conduction band depend very strongly on their concentration in a nonequilibrium superconductor, only very low concentrations $c << 1$ are considered in this analysis and ion-ion interaction is accordingly assumed to be negligible. The ionic nonequilibrium subsystem is, moreover, assumed to only slightly influence the quasiparticle excitations "heated up" by the tunneling source. In this case the presence of such a paramagnetic impurity can be assumed to change the density of states of quasiparticles and that of Cooper pairs as well as the width of the superconductor energy gap. This assumption is used for describing the electronic part of the equation of kinetics for rare-earth ions. Derivation of this equation requires determination of the Green-Keldysh nonequilibrium functions, these functions for rare-earth ions in the pseudofermion representation being obtained from the applicable Hamiltonian. Following the solution of coupled equations for the frequency and the order parameter in the one-particle electronic Green functions for the superconductor, both having been renormalized by interaction of the latter with rare-earth ions, subsequent change to and integration of the Green-Gorkov-Eilenberger-Eliashberg functions yield an equation of kinetics for the population of energy levels of rare-earth ions, a paramagnetic one with a singlet ground level, an equation which takes into account the imbalance between electron and hole branches of the spectrum. An equation of kinetics for the distribution function of quasiparticle excitations $n(+/-\varepsilon)$ in the superconductor is obtained as it is obtained in the case of a pure superconductor, but in the relaxation time approximation for the collision integral and taking into account the presence of rare-earth ions. As a simple example, a symmetric SIS sandwich with paramagnetic rare-earth impurity ions in the two layers of high-T_c superconductor material is selected. The corresponding

two pairs of coupled equations have been solved by the iteration method for the steady-state population of the singlet ground level of these ions, to facilitate a numerical evaluation of its dependence on the voltage across the sandwich and on the Cooper pair annihilation parameter. The author thanks A. A. Mitrofanov for assisting with numerical calculations. Figures 2; references 17.

Feasibility of Experimental Validation of Nyquist's Quantum-Theoretical Formula for Fluctuation Noise

927J0003B Moscow DOKLADY AKADEMII NAUK SSSR in Russian Vol 317 No 2, Mar 91 pp 348-350

[Article by G. T. Petrovskiy, corresponding member, USSR Academy of Sciences, and N. V. Starostin, State Institute of Optics imeni S. I. Vavilov, Leningrad]

UDC 536.75:530.145

[Abstract] Fluctuation noise in electrical oscillators and rare-earth crystals is considered from the quantum-theoretical standpoint, Nyquist's classical formula (PHYSICS REVIEW Vol 32 No 1, 1928) being appropriately modified by equating the average energy in such a system not to kT/2 but to $[h\omega/2 + h\omega/\exp(h\omega/kT) - 1]/2$ (k - Boltzmann constant, h - Planck constant, ω - frequency). The new formula needs to be experimentally validated, the feasibility of this having been established by analysis of experimental data: 1) on the spectral density of Nyquist current noise in a tuned oscillatory electric circuit coupled to a system of nuclear spins and on temperature-independent weak voltage fluctuations proportional to $N^{1/2}/\mu$ (F. Bloch, PHYSICS REVIEW Vol 70 No 2, 1946, μ - magnetic moment of spin) induced by a specimen with N spins inside a solenoid spontaneously injecting them into that circuit, measurements having been made (T. Sleator, E.I. Hahn, C. Hilbert, and J. Clarke, PHYSICS REVIEW LETTERS Vol 55 No 17, 1985) with $NaClO_3$ nuclear quadrupole resonance frequency for ^{35}Cl nuclei; 2) on magnetooptically recorded noise resonance in a system of paramagnetic atoms; 3) on excitation of a rare-earth concentrate crystal by intense (allowed in the dipole approximation) f-d transitions for laser spectroscopy, faint (forbidden in the dipole approximation) f-f transitions being here the luminescent ones. More recently, moreover, changes in the diamagnetic Meissner state of superconductor materials including those in the high-T_c class have been utilized for high-precision recording of fluctuation noise by either the circuital method or the optical method. Validation of Nyquist's quantum-theoretical formula thus hinges on a practical implementation of the scientific techniques. References 11.

Thermal Conductivity Anomaly Near Second Order Phase Transition Point in Uniaxial Ferroelectric

927J0032A Leningrad FIZIKA TVERDOGO TELA in Russian Vol 33 No 2, Mar 91 pp 691-701

[Article by B. A. Strukov, A. A. Belov, Ye. L. Sorokin, Moscow State University imeni M. V. Lomonosov]

[Abstract] The history of heat transfer investigations in ferroelectric crystals since 1960 is reviewed and the problem of measuring the temperature dependence of thermal conductivity of triglycinsulfate—a high-quality model ferroelectric crystal with a second-order phase transition accompanied by the appearance of spontaneous polarization along the [010] axis near a 49°C temperature is formulated in order to ascertain the character of critical thermal conductivity anomaly. To this end, precision measurements of the temperature dependence of the thermal conductivity of uniaxial ferroelectric crystals of triglycinsulfate with a second-order phase transition are taken in the 300-340K temperature range. A thermal conductivity minimum is discovered at the Curie point. The resulting data make it possible to attribute the considerable discrepancy in temperature dependence measurements to the effect of the crystal imperfection and impurities on the measurement results. Future studies of the effect of electric field on the temperature dependence of the ferroelectrics' thermal conductivity are planned. Figures 3; tables 1; references 16: 4 Russian, 12 Western.

Electrostatic Model of Spherical Lightning

927J0009D Leningrad PISMA ZHURNAL TEKHNICHESKOY FIZIKI in Russian Vol 17 No 7, 12 Apr 91 pp 34-37

[Article by I. V. Zaytsev and S. V. Zaytsev]

[Abstract] A model of a spherical lightning in the air is constructed by hypothetically treating it as an analog of a soap bubble with a positive in water. The condition for its stability is established in terms of a balance of two forces acting on the surface: tension by internal pressure of the electrostatic field proportional to the electric field intensity squared and compression by external pressure of the ambient medium proportional to the concentration of polarized surrounding molecules. The condition for equilibrium is determined from the equation $\varepsilon E_0^2/2 = p_{M\infty}\exp[E_0^2/2kT(\alpha + p_0^2/3kT]$ (ε - dielectric permittivity of water, E_0 - electric field intensity at bubble surface, p - ambient pressure, p_∞ - pressure far away from bubble, P_0 - constant dipole moment of water molecule, T - ambient temperature, k - Boltzmann constant), this equation having two solutions corresponding to two magnitudes of the electric field intensity. The first solution corresponds to equilibrium at some lower electric field intensity and pressure, this equilibrium being unstable under small perturbations of the bubble surface. The second solution corresponds to equilibrium at some higher electric field intensity and pressure. For a spherical bubble with a radius of 7 cm at a temperature of 300 K this higher electric field intensity of 5.5 GV/m is insufficient for autoionization of water molecules and this higher pressure of 0.23 GN/m^2 is, according to Paschen's law, insufficient for electric breakdown. Breakdown is possible only at some distance from the bubble surface, dipole-dipole repulsion evidently preventing vapor condensation but molecules possibly forming radial chains. The energy of a spherical lightning is estimated on this basis, considering that it is the sum of four parts: energy of the electrostatic field (580 kJ, corresponding to charge of 3 mC), energy acquired by constant dipoles in this field, energy expended on negative polarization, and work done on compression of the gas. Further refinement of this model is expected to make it cover all properties of a spherical lightning. Figures 1; references 5.

END OF FICHE

DATE FILMED

28 Feb 1992